2014

Reconsidering the Model of Trim5α Assembly: The Role of the Linker2 (l2) Region in Trim5α Assembly

Laura Johnsen
Loyola University Chicago

LOYOLA UNIVERSITY CHICAGO

RECONSIDERING THE MODEL OF TRIM5α ASSEMBLY: THE ROLE OF THE LINKER2 (L2) REGION IN TRIM5α ASSEMBLY

A THESIS SUBMITTED TO

THE FACULTY OF THE GRADUATE SCHOOL

IN CANDIDACY FOR THE DEGREE OF

MASTER OF SCIENCE

PROGRAM IN MICROBIOLOGY AND IMMUNOLOGY

BY

LAURA JOHNSEN

CHICAGO, ILLINOIS

DECEMBER 2014

ACKNOWLEDGEMENTS

I would like to thank everyone who has helped me make this thesis possible. My mentor, Dr. Edward Campbell, has always encouraged me to think deeply and logically about scientific problems, and he really taught me the value of how much hard work can pay off. The training and support provided by Dr. Campbell has strengthened my confidence and helped me develop into a young, ambitious scientist. I would also like to thank the Department of Microbiology and Immunology for giving me numerous opportunities to publicly present my research and receive feedback from other faculty and students in the department.

I also thank my friends for always supporting me and helping me through the graduate school process by constantly reminding me how proud they are of me. I also thank my parents for always being there for me and supporting me. They continuously made me believe in my academic success and myself. Without their support, I would not be where I am today. Additionally, I thank the rest of my family for their love and support as well as their interest in my success.

There are things known and things unknown and in between are the doors.

Jim Morrison

TABLE OF CONTENTS

LIST OF FIGURES

ABSTRACT

The TRIM5α protein from rhesus macaques ($TRIM5\alpha_{rh}$) exhibits a remarkable ability to potently inhibit infection by Human Immunodeficiency Virus Type-1 (HIV-1). Extensive studies have shown that TRIM5α is capable of self-associating at many levels, eventually leading to the formation of a hexameric assembly that can superimpose on the hexameric lattice of the HIV-1 capsid. The mechanism underlying the self-association of TRIM5α and the molecular determinants of self-association remain to be completely understood. In this study, we show that the Linker 2 (L2) region of $TRIM5_{rh}$ is important for dimerization and higher order self-association, both of which are independent processes. Additionally, fluorescence resonance energy transfer (FRET) analysis suggests that an antiparallel dimer configuration is the basic unit of TRIM5α, consistent with the recently published crystal structure of the CCL2 region of TRIM25 by Sanchez et al. We propose a homology model of the CCL2 fragment of TRIM5α based on the structure of the TRIM25 CCL2 region. In this model the Helix 3 of the L2 region folds back onto Helix 1 (CC domain), possibly ensuring correct binding of the SPRY domain to the HIV-1 core. These studies reveal previously unknown determinants in the L2 region that govern self-association of TRIM5α.

CHAPTER 1

INTRODUCTION

Acquired Immunodeficiency Syndrome (AIDS) has taken over thirty-six million lives since its discovery in 1981, and an additional 33.4 million people are currently infected worldwide (CDC). AIDS, an immune system disease of humans, can be characterized by a below average $CD4^+$ T cell count. Once this occurs, the immune system can no longer fight off infections and the body can succumb to opportunistic pathogens. Human Immunodeficiency Virus Type 1 (HIV-1) is a lentivirus that can lead to AIDS by infecting a variety of critical immune cells; including $CD4^+$ T cells, dendritic cells, and macrophages. This generally leads to fatality by overpowering the immune system leading to AIDS.

HIV-1 Structure and Genome

HIV-1 is a lentivirus belonging to the retroviridae family that predominantly infects $CD4^+$ T helper cells as well as other immune cells such as macrophages. Lentiviruses manifest slowly into disease and are capable of integrating into the host cell genome as a provirus that can remain dormant for years in resting $CD4^+$ memory T cells. HIV-1 virions are about 100 nm in diameter and generally spherical, coated with a viral envelope or membrane composed of phospholipids (Figure 1b). The virus carries two copies of positive single-stranded RNA, approximately 10 kilobases in length, which code for nine open reading frames (ORFs) and fifteen proteins (Figure 1a). The three

polyproteins, which can then be cleaved by the viral protease encoded within the Pol polyprotein. Env is cleaved by the viral protease into two glycoproteins: the transmembrane gp41 (TM) and gp120 (SU) located on the surface of the virion. These function to bind to receptors on the infected cell to facilitate fusion of viral and cellular membranes. During viral maturation, the viral protease cleaves Pol away from the Gag-Pol precursor and then further cleaves the Pol polypeptide into three proteins: protease (pro, p10), reverse transcriptase (RT, p50), and integrase (IN, p31). Pro is required to cleave Gag and Gag-Pol polyproteins during virion maturation. RT makes a double-stranded DNA copy of the two genomic RNA strands, and encompasses RNase H activity to eliminate the RNA strand from the first DNA strand, permitting generation of a complementary strand of DNA (cDNA). IN mediates the insertion of the HIV-1 provirus into the host cell genome through three critical functional enzymes: exonuclease, endonuclease, and ligase. Gag is cleaved into four proteins: matrix (MA, p17), capsid (CA, p24), nucleocapsid (NC, p9), and p6 that make up the viral core. MA lines the interior of the viral membrane to increase virion stability. Assembled from 250 hexamers and 12 pentamers, CA forms a hexameric lattice composed of about 1500 copies of CA that help make up the conical core around the viral RNA[1, 2]. The NC forms a stable complex with the viral RNA for protection. All of the above mentioned structural proteins facilitate early events during infection.

In addition to structural proteins, HIV-1 also encodes regulatory proteins (Tat and Rev) and accessory proteins (Vpu, Vpr, Vif, and Nef) that interact with the human host. Tat is a transcriptional transactivator expressed early in infection that recognizes a

transactivator response element (TAR) in the 5’ hairpin structure of the viral RNA to begin complex formation for transcription initiation. Rev is an RNA binding protein that binds to the Rev response element (RRE) to regulate splicing and transport of viral RNA by allowing unspliced transcripts to move from the nucleus to the cytoplasm for translation and packaging of the virus. Vpu helps weaken interactions between viral glycoproteins and host cellular receptors to assist in virus escape. Vpr has been shown to facilitate the movement of the viral genome into the nucleus upon infection. Vif destroys host cellular proteins to increase production of infectious virions. Finally, Nef is thought to serve many purposes including: CD4 expression downregulation, perturbation of T cell activation, and infectivity enhancement.

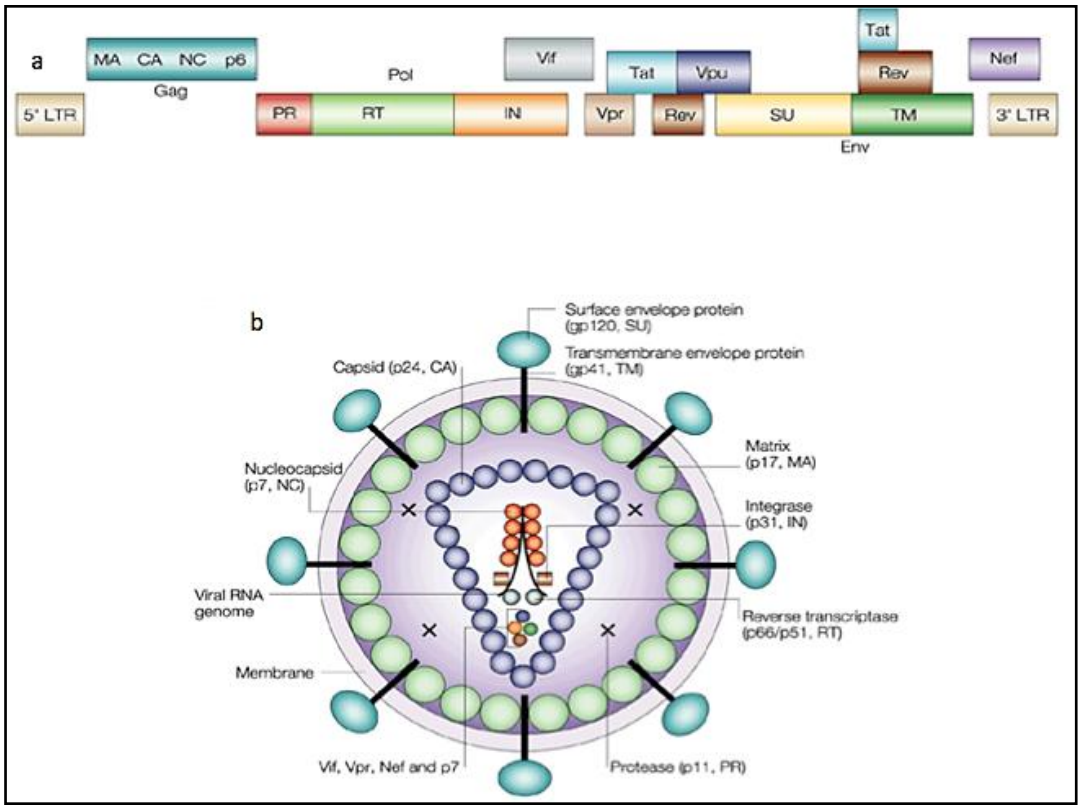

Figure 1: HIV-1 structure and genome. A) Genomic organization of the HIV-1 genome. B) Structural organization of an HIV-1 virion. Reprinted with permission from [3].

HIV-1 Life Cycle

Viral Entry

The HIV-1 envelope spikes, gp41 and gp120, initiate viral entry into $CD4^+$ T cells or other immune cells expressing CD4 (macrophages and dendritic cells). A primary interaction between gp120 and CD4 promotes conformational changes that expose binding sites on gp120 for a second cell surface molecule known as chemokine receptor 5 (CCR5) (Figure 2-step 1)[4]. Subsequently, the fusion peptide that is part of the gp41 N-terminus is inserted into the host cell membrane to allow fusion between viral and cellular membranes (Figure 2-step 2).

Uncoating

Uncoating is the process by which the viral core, which houses the ribonucleoprotein (RNP) complex, begins to dissociate allowing the viral RNA to enter the cytoplasm of the host cell (Figure 2-step 3). The exact details of uncoating remain somewhat unclear in the field of HIV, however uncoating is essential for reverse transcription to occur.

Reverse Transcription and Integration

The viral enzyme, RT, converts viral RNA into cDNA using host nucleotides (Figure 2-step 4). Since RT has very little to no proofreading ability, many errors result from this process. The end result from reverse transcription is the pre-integration complex (PIC). The PIC has been shown to be associated with the viral proteins NC, MA, RT, IN, and Vpr[5-7].

The nascent viral DNA can then be carried into the host cells' nucleus through the nuclear pore complex (NPC) (Figure 2-step 5). Viral CA has been demonstrated to be a key determinant in nuclear import of the viral PIC, suggesting a connection between uncoating and nuclear import[8]. In addition, several cellular proteins (Nup153, Nup358, and TNPO3) have been shown to interact with HIV-1 CA to facilitate nuclear import of the PIC[9-12].

The viral IN facilitates the joining of HIV DNA with host cell DNA forming an integrated provirus (Figure 2-step 6). IN does this by essentially nicking the DNA to allow for HIV-1 to insert itself, establishing life-long infection. The provirus may 'hide' and remain inactive (or latent) in the host cell genome for extended periods of time.

Transcription and Translation

The viral Tat protein is essential for successful transcription of the integrated provirus (Figure 2-step 7). Tat operates by recruiting host cellular factors such as RNA Pol II to the TAR element to facilitate transcription elongation. Once viral DNA is transcribed into mRNA, it is carried out of the nucleus by cellular proteins and the viral protein Rev (Figure 2-step 8). Short mRNAs can easily move out of the nucleus through the use of CRM-1, a host nuclear export protein, while longer mRNAs require Rev. These mRNAs then serve as templates for translation through the use of the host cell translation machinery (Figure 2-step 9).

Assembly and Budding

Viral proteins gather at the cell surface along with viral genome-length RNA for assembly of new viral particles (Figure 2-step 10). Particle budding, facilitated by the

cellular endosomal sorting complex required for transport (ESCRT) machinery (Figure 2-step 11), and release (Figure 2-step 12) is followed by maturation mediated by the viral protease (Figure 2-step 13) to create a new virion for infection to spread to other $CD4^+$ T cells.

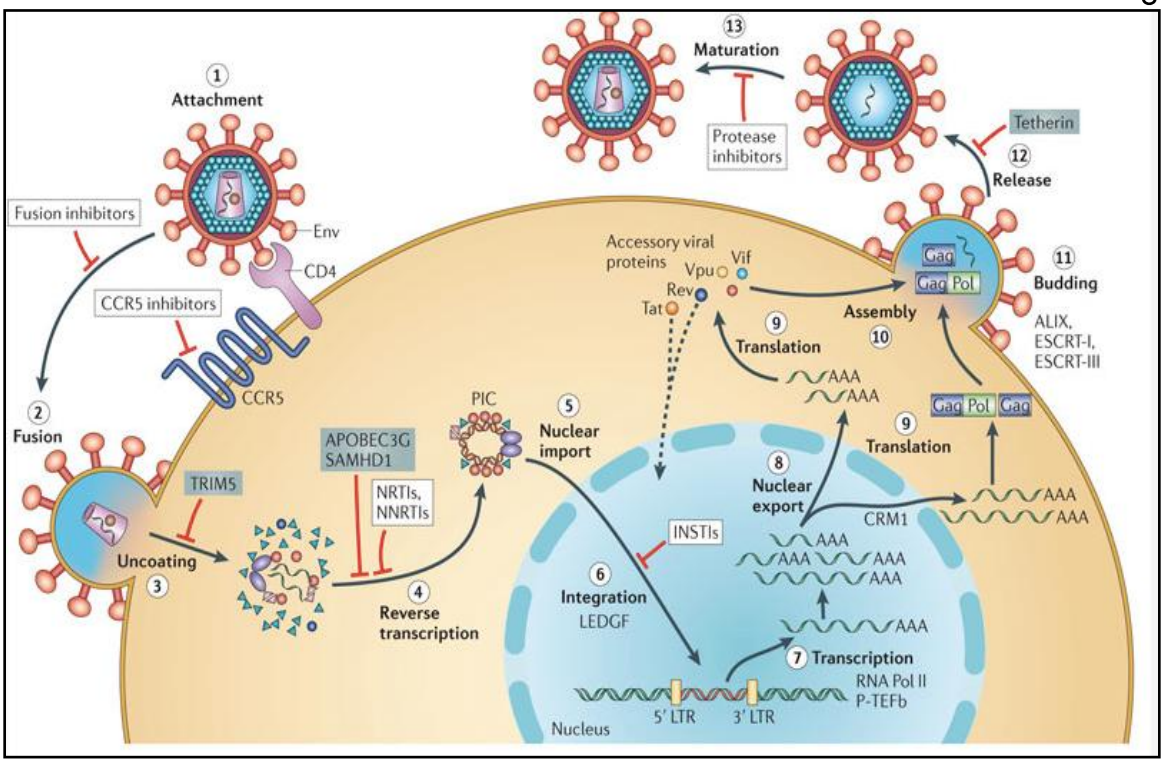

Figure 2: HIV-1 viral life cycle, antiretroviral therapeutics, and cellular restriction factors. Reprinted with permission from[4].

Antiretroviral therapeutic targets

The HIV-1 life cycle provides several points of intervention, however only four of the above-mentioned steps have been the targets of various drugs approved in the United States to administer to HIV positive individuals. Since the initiation of highly active antiretroviral therapy (HAART), morbidity and mortality accompanying HIV-1 infection and AIDS has dwindled[13]. HAART typically includes a combination of three drugs to suppress viral replication and reduce viral loads in the plasma to allow the immune system to rebuild[14-16]. The success of HAART results in part due to the diminished likelihood of choosing virus clones with several mutations and conferring resistance to a three-antiretroviral-drug regimen[17]. Nevertheless, as the virus continues to evolve and escape, novel HIV-1 treatments will continuously be desired.

There are currently twenty-four Food and Drug Administration (FDA)-approved drugs available that can be divided into six classes based on their mechanism of action: (1) nucleoside-analog reverse transcriptase inhibitors (NRTIs), (2) non-nucleoside reverse transcriptase inhibitors (NNRTIs), (3) integrase inhibitors, (4) protease inhibitors, (5) fusion inhibitors, and (6) coreceptor antagonists[17]. The HAART regimen usually comprises an NRTI, NNRTI, and a protease inhibitor[4]. When only one of the viral proteins is targeted, the virus can simply attain mutations to acquire resistance to that drug. However, the use of combinational drug therapy targeting multiple viral proteins reduces the possibility that the virus will develop resistance.

Viral Entry and Fusion Inhibitors (Figure 2-Step 1 and 2)

HIV-1 entry and fusion inhibitors work by inhibiting the interaction between envelope glycoproteins and the target cell. Crystallographic studies have suggested that upon CD4 receptor engagement, gp120 undergoes tremendous conformational modifications, and CD4 binds gp120 between the inner and outer domains in a conserved hydrophobic pocket[18]. Therefore, small molecule inhibitors that mimic CD4 and extend further into the conserved binding cavity on gp120 may increase the affinity for gp120 leading to the production of clinically suitable inhibitors[19].

Generally, antibodies against gp120 fail to neutralize HIV-1 and are strain specific. However, one group of researchers was able to redesign gp120 to disguise sites external to the CD4-binding site[20, 21]. Using this construct along with peripheral mononuclear cells from AIDS patients, Wu et al. isolated B cell clones that created antibodies capable of broad neutralizing activity by engaging the CD4-binding site.

Additionally, peptides derived from gp41 N- or C-terminal sequences that disrupt membrane fusion elicit antiviral activity[22, 23]. Enfuvirtide (Fuzeon) derived from the C-terminus has been approved for therapeutic use, however its use is restricted due to the requirement for multiple daily injections of the drug. Resistance mutations in gp41 have also limited the use of Fuzeon clinically.

Reverse Transcription Inhibitors (Figure 2-Step 4)

NRTIs and NNRTIs inhibit DNA polymerization and are a part of HAART. NRTIs mimic natural 2’-deoxyribonucleoside 5’-triphosphates (dNTPs) to become incorporated into the viral DNA by RT[4]. They act as chain terminators because NRTIs do not have the 3’-hydroxyl group required for successive nucleotide incorporation.

Unfortunately, viral resistance to NRTIs is common. Thymidine analogues, such as 3'-azido-3'-deoxythymidine (AZT), have allowed for mutant RTs to develop that acquired the capacity to eliminate the incorporated drug from the primer strand[24, 25].

NNRTIs act as allosteric inhibitors to induce conformational changes that form a flexible binding pocket in the RT active site[26, 27]. Drug binding likely arises as a result of interactions between aromatic side chains of Tyr181 and Tyr188 and the NNRTI, such as nevirapine[26]. Viral resistance has been associated with mutations that restrict the movement of Tyr188[4]. Newer NNRTIs, etravirine and rilpivirine, contain intrinsic flexibility that allows for high-affinity binding to the mutant RT that has evolved from first-generation NNRTIs[28].

IN Strand Transfer Inhibitors (INSTIs) (Figure 2-Step 6)

Raltegravir is a clinically approved HIV-1 INSTI that inhibits DNA strand transfer activity[29]. INSTIs engage the bound metal ions in the IN active site to somewhat effect their positioning, and the halogenated benzyl groups of INSTIs interact with the viral DNA and IN to eject viral DNA from the active site[29, 30]. These types of inhibitors can also sterically prevent target DNA binding to the IN active site[31, 32].

Lentiviruses prefer to integrate within active genes because of an interaction between IN and LEDGF, a cellular chromatin-binding protein. Recently developed HIV-1 IN inhibitors, known as LEDGINs, can mimic this interaction and impede protein-protein binding[4, 33].

Protease Inhibitors (Figure 2-Step 13)

PR inhibitors are competitive inhibitors because they can bind to the active site of PR and inhabit the inhibitor envelope[4]. These drugs are designed to bind explicitly within the PR binding groove and only make contact with residues absolutely required for PR function. The idea is that resistance mutations in the viral PR would be highly unfavorable because any mutation would abolish PR functional activity[4].

Cellular Restriction Factors of HIV-1

In addition to the clinically available drug therapies targeted at various steps of the viral life cycle, complex organisms have evolved a collection of dominant, constitutively expressed genes that suppress or block HIV-1 infection. These activities fall outside the established definitions of innate and adaptive immunity, but provide 'intrinsic immunity' to allow effective defense from viral infection[34]. Restriction factors are largely responsible for this intrinsic immunity by acting as the front line of host defense against viral infection. The initial evidence of cellular restriction factors originates in mice when Friend virus susceptibility factor 1 (Fv1) was discovered as an inhibitor of murine leukemia virus (MLV)[35]. Eventually, similar activities were discovered in other mammals, including humans. In humans, restriction factor 1 (Ref1) was found to inhibit N-tropic MLV (N-MLV) infection in a manner very similar to Fv1-mediated restriction of MLV in mice[36].

A central idea to the biology of restriction factors is that HIV-1 usually escapes their strong inhibitory activities in human cells, thereby permitting virus replication to continue. In contrast, HIV-1 replication in nonhuman cells is generally limited by restriction factors, marking these proteins as vital elements to viral host range and cross-

species transmission[37]. Since their initial discovery, several restriction factors have been identified for HIV-1, such as TRIM5α, APOBEC3G, SAMHD1, and tetherin.

APOBEC3G (Figure 2-Step 4)

The discovery of Apolipoprotein B mRNA-editing enzyme, catalytic polypeptide-like 3G (APOBEC3G or A3G) arose as a result of understanding the function of the viral protein Vif, which is required for HIV-1 replication in primary cells. Comparative transcriptomics revealed that the human gene *APOBEC3G* could suppress the replication of *vif*-deficient HIV-1[38]. A3G has cytidine deaminase activity that edits cytidines to uridines to manipulate the nucleotide sequence[37]. In the absence of Vif, A3G becomes packaged into nascent HIV-1 virions and is transported to new target cells by associating with the viral RTC to deaminate cytidine residues in newly synthesized viral cDNA, causing guanosine-to-adenosine hypermutation of the viral positive strand[39].

The molecular 'arms race' between virus and host allowed HIV-1, and other lentiviruses, to acquire Vif, which counteracts A3G activity by recruiting A3G for proteasomal degradation. This action results in the inability for A3G to be packaged into newly assembling virions. The species-specific regulation of A3G by HIV and simian immunodeficiency virus (SIV) Vif proteins is attributed to differences in amino acid sequence of human and African green monkey (AGM) A3G, thus permitting recognition by SIV_{AGM}, but not HIV-1, Vif[40, 41]. It remains a challenge to tackle if disparity in APOBEC3 can impact the course of HIV-1 infection in humans, however some findings have proposed that higher levels of A3G, and the less potent APOBEC3F (A3F), expression are associated with medical advantages[40].

SAMHD1 (Figure 2-Step 4)

The inhibition of HIV-1 infection in myeloid cells involves the cellular sterile alpha motif domain HD domain-containing protein 1 (SAMHD1)[42, 43]. SAMHD1 is highly expressed in myeloid-lineage monocytes, such as macrophages and dendritic cells. SAMHD1 limits viral replication by hydrolyzing and reducing intracellular dNTPs, which are essential for viral DNA synthesis[44]. Vpx and Vpr proteins of HIV-2 and SIV from macaques (SIV_{MAC}) and African green monkeys (SIV_{AGM}) have been shown to offset SAMHD1-mediated restriction of HIV-1 by targeting SAMHD1 for ubiquitin-proteasome-dependent degradation[44-47]. HIV-1 does not contain a protein that can antagonize SAMHD1, however HIV-1 can still replicate, although less efficiently, due to the capacity of its RT to function under environments of low dNTP availability[44]. HIV-1 stealthily and slowly replicates in non-cycling myeloid cells and sufficiently allows for further transmission to activated cells[48]. This covert replication might avoid recognition by the immune system.

Tetherin (Figure 2-Step 12)

Tetherin (also known as CD317 and BST2) was identified based on studies of the Vpu accessory protein. In the absence of Vpu, HIV-1 is sensitive to a tethering mechanism that traps nascent virions on the surface of infected cells and internalizes them into endosomes[49-51]. Tetherin is astonishingly tolerant of mutations, including replacement of entire tetherin domains with protein domains parallel in structure but not sequence[52]. Tetherin has also been found in virions suggesting that either or both membrane anchors are inserted into the lipid envelope of budding virions as they appear

from infected cells. Additionally, tetherin colocalizes with virions on the cell surface[52-56]. The tetherin antagonist, HIV-1 Vpu, lessens the level of tetherin at the cell surface by causing its internalization or delaying its advancement through the secretory pathway[51, 57, 58]. Studies have also shown that Vpu can decrease the overall steady-state level of tetherin in cells when overexpressed[59]. The HIV-1 Vpu is species-specific in that it is unsuccessful against tetherins from other animals, such as monkeys[60, 61].

TRIM5α (Figure 2-Step 3)

TRIM5α is an ~500 amino acid protein that is in the tripartite motif (TRIM)-containing family of proteins[37]. It restricts by acting, in a species-specific manner, on retroviral capsids following their entry into the cytoplasm. Generally, TRIM5α proteins weakly hinder retroviruses in the same host species but not other species. For example, human TRIM5α (TRIM5α_{hu}) can inhibit N-MLV but not HIV-1, whereas TRIM5α from old world monkeys can inhibit HIV-1[62-65]. At its C-terminus, TRIM5α has a B30.2/SPRY domain that directly binds the retroviral capsid. Variable loops within the SPRY domain have been shown to be vital determinants of antiretroviral specificity, and even single amino acid substitutions in one of these segments of primate TRIM5α can modify the capability to identify HIV-1 and SIV strains[66-69]. Retrotransposition events have placed cyclophilin A (CypA) into the TRIM5 locus, replacing the SPRY domain, of owl monkeys creating TRIMCyp[70-72]. TRIMCyp also potently inhibits HIV-1 infection through capsid binding and disruption[73-76].

Due to limited availability of experimental techniques to study the post entry phase of HIV-1 where TRIM5α acts, it remains poorly understood how TRIM5-mediated

restriction occurs mechanistically. What is known is that TRIM5α directly binds incoming HIV-1 capsids within fifteen minutes after the virus enters the cell[66, 77]. TRIM5α forms hexameric crystalline arrays in the presence of a higher-order six-fold lattice of HIV-1 capsid[78]. This capsid-patterned oligomerization may trigger HIV-1 restriction by rhesus TRIM5α (TRIM5α_{rh}) through a pattern recognition mechanism[79].

TRIM5α

Protein Domains and their function

The human genome contains roughly seventy genes of the TRIM family[80-83]. Most TRIM proteins are defined by the presence of the tripartite motif: a really interesting new gene (RING) domain, one or two B-Box domains, and a coiled-coil (CC) domain[81]. The tripartite motif is highly conserved, so the functional differences amongst TRIM proteins can be accredited to their C-terminal domains. The most common C-terminal domain is the PRY/SPRY, or B30.2 domain[81]. A depiction of TRIM5α_{rh} is shown in figure 3.

The RING domain is present at the N terminus of TRIM5α that contains a putative E3 ubiquitin ligase activity essential for TRIM5α autoubiquitination and HIV-1 restriction[84]. The RING finger motif is a zinc-binding domain and defined by a distinctive linear sequence of conserved cysteine and histidine amino acids[85][84, 86]. Substitution of alanine for the conserved cysteine15 in the RING-finger domain to generate a C15A TRIM5α mutant depleted *in vitro* self-ubiquitination activity of TRIM5α[84, 87]. Removal of the RING domain has been shown to affect proteasome interactions by postponing the block in virus replication until after reverse transcription

has happened[88].

The B-box domain is another zinc-binding motif that occurs in two similar orientations (B-box 1 and B-box 2) except for a distinct pattern of cysteine and histidine residues[81]. TRIM5α only contains the B-box 2 domain, which is unique to members of the TRIM protein family[81]. The B-box 2 domains of numerous TRIM proteins, including TRIM5α, have been linked to protein-protein interactions, multimerization, and subcellular localization[89]. Disruption of TRIM5α_{rh} or TRIM5α_{hu} B-box 2 domain antagonizes the ability of these proteins to mediate retroviral restriction[66, 90, 91]. The B-box domain of TRIM5α promotes cooperative CA binding by mediating TRIM5α self-association[89].

The coiled-coil (CC) domain has been identified as important for the formation of homo-oligomers, which is essential for antiviral activity[92]. The CC domain is chiefly comprised of alpha helices and is necessary for the development of TRIM5 dimers, which form the building blocks for higher order assembly[81, 93]. Deletion of the CC region has also been shown to avoid stable binding of the retroviral CA protein[77].

The C-terminal SPRY domain of TRIM5α plays a crucial role in retroviral restriction by identifying certain determinants in the retroviral capsid and directly binding the capsid[65]. The SPRY domain has three variable loops evolved to recognize specific sites in the retroviral capsid[67, 68, 94, 95]. This results in species-specific retroviral restriction. Yap et al. demonstrated that a single amino acid change in the SPRY domain of TRIM5α_{hu} is sufficient to gain restriction of HIV-1 in a similar manner as TRIM5α_{r}

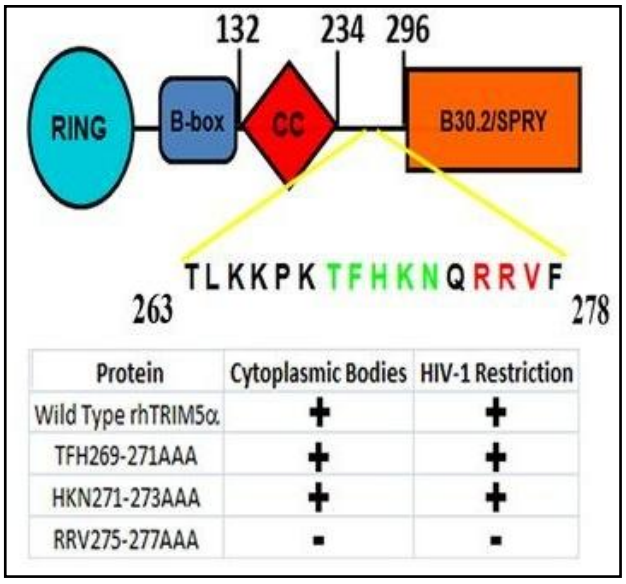

Protein	Cytoplasmic Bodies	HIV-1 Restriction
Wild Type rhTRIM5α	+	+
TFH269-271AAA	+	+
HKN271-273AAA	+	+
RRV275-277AAA	-	-

Figure 3: Schematic representation of TRIM5α_{rh}. (Above) Representation of the various domains of TRIM5α_{rh}: the RING, BBox, coiled-coil (CC), and B30.2/SPRY with the indicated amino acid positioning of the Linker 2 (L2) region (amino acids 234-296). A zoomed in portion of the L2 region (amino acids 263-278) represents the site of triple alanine mutagenesis. (Below) The abilities of the indicated WT or L2 mutants to elicit cytoplasmic body formation and mediate HIV-1 restriction.

Cytoplasmic Bodies and the Linker 2 Region

TRIM5α has been shown to localize to cytoplasmic growths of protein termed 'cytoplasmic bodies'[65, 96], which functionally, in terms of restriction, remain relatively unclear. Two previous studies have found that cytoplasmic body localization is not required for restriction[66, 97]. In contrast to these studies, Campbell et al. has observed that cytoplasmic bodies are dynamic, trafficking on microtubules, and form around individual HIV-1 virions in restricted cells[96, 98]. These studies would alternatively propose that cytoplasmic bodies are significant for interactions between TRIM5α and incoming retroviral capsids during restriction.

Sastri et al. utilized a variety of TRIM5α truncation mutants to locate regions required for cytoplasmic body localization[99]. From these studies the region between the CC and SPRY domains, the linker 2 (L2) region, were found to contain residues that mediate cytoplasmic body formation. Additionally, deletion of the L2 region of full-length TRIM5α_{rh} inhibited the formation of cytoplasmic bodies and HIV-1 restriction[99]. Furthermore, as shown in figure 3, scanning alanine mutagenesis identified two segments of amino acids, KPK266-268AAA and RRV275-277AAA, in the L2 region that cause a diffuse localization of TRIM5α and are unable to restrict HIV-1 compared to WT TRIM5α_{rh}[99]. The other two mutants, TFH269-271AAA and HKN271-273AAA have recently been shown by our lab to form more cytoplasmic assemblies per cell than wild-type TRIM5α_{rh}[100]. It appears that residues within the L2 region facilitate self-association of TRIM5α_{rh}, and this ability to self-associate is important for restriction. Indeed, previous studies have demonstrated that the L2 region

affects the ability of TRIM5α_{rh} to multimerize in biochemical crosslinking experiments[76, 90, 92, 101].

Self-association of TRIM5α

Self-association of TRIM5α involves dimerization, higher-order multimerization, and assembly[78, 92, 101], all of which are necessary for retroviral restriction mediated by capsid recognition.

Initially, it was thought that TRIM5α forms trimers[101], however more recent studies suggest that dimerization is more likely[102]. These studies utilized a recombinant TRIM5α_{rh} protein (TRIM5-21R) containing the RING domain from the related TRIM21 protein to demonstrate that chemically cross-linked dimeric TRIM5-21R bound HIV-1 CA-NC assemblies better than monomeric TRIM5-21R[102, 103]. This direct binding to retroviral capsid-like complexes occurred in the absence of other mammalian proteins. The CC domain is required for the formation of TRIM5α dimers[66, 81], contributing to the avidity of TRIM5α for the HIV-1 CA[62, 64, 70, 71, 104]. Deletion of the TRIM5α_{rh} CC disrupts the interaction with HIC-1 CA-NC assemblies and loses the ability to act as a restriction factor[77].

The B-box 2 domain has been shown to promote higher order self-association between preformed TRIM5α dimers that is required for retroviral CA binding and restriction[76, 89-92, 102, 103, 105-107]. Indeed, it has been shown that mutations in the B-box 2 region of TRIMα decreased binding to HIV-1 CA suggesting that these modifications affect capsid recognition by positioning or conformation of the SPRY domain[106]. On the other hand, B-box 2 mutations in TRIMCyp abrogated HIV-1

restriction and CA binding compared to wild-type TRIMCyp[106]. Furthermore, a recombinant protein containing the cyclophilin A domain from owl monkey TRIMCyp in place of the SPRY domain of TRIM5α_{rh} was created to determine if CA recognition differences between TRIM5α and TRIMCyp was due to alterations between the TRIMdomains[106]. B-box 2 domain mutations were introduced into this chimeric protein however these did not affect the ability to bind HIV-1 CA-NC assemblies[106]. CypA has a higher affinity for the HIV-1 CA as compared to the SPRY domain, suggesting that the B-box 2 domain is required to increase the interaction between the SPRY domain of TRIM5α_{rh} and HIV-1 CA. Additional studies have identified a hydrophobic patch on the B-box 2 domain, and changes in this patch or the flanking arginine 121 inactivated TRIM5α_{rh}-mediated HIV-1 restriction[105]. The loss of restriction observed in this study was linked with higher-order self-association and HIV-1 CA binding affinity. The RING domain has also been shown to be required for TRIM5α higher-order self-association; ΔRING-TRIM5α_{rh} can form dimers but cannot self-associate in co-immunoprecipitation assays with wild-type TRIM5α_{rh}[108]. Additionally, the L2 region may contribute to the effectiveness of higher-order self-association since multiple L2 mutations were found to dimerize well but had diminished efficiencies in higher order association with wild-type TRIM5α_{rh}[108]. The SPRY domain is not required for higher order self-association[89].

The role of CC and L2 regions in TRIM5α Assembly

The finding that scanning alanine mutagenesis of the L2 region of TRIM5α can increase or decrease assembly proposes that these mutations may be changing secondary

structural elements. Our lab has recently demonstrated that the α-helical content of the L2 region correlates to the ability to form cytoplasmic assemblies and restrict HIV-1[100]. The above-mentioned L2 mutations that displayed heightened cytoplasmic body formation compared to wild type had higher α-helical contents than wild type[100]. In contrast, mutations with decreased cytoplasmic body formation showed lower α-helical contents than wild type. These findings were based on Circular dichroism (CD) studies of both the CC and L2 regions. CD analysis utilizing synthetic peptides comprising only the L2 region did not reveal α-helical secondary structure except in the presence of 10% trifluoroethanol (TFE), which can stabilize α-helical structures, where the α-helical content of L2 peptides correlated with their ability to assemble and restrict infection, similarly to CCL2[100]. This implies that the L2 region of TRIM5α_{rh} is not inherently α-helical in the absence of the CC domain, proposing that the presence of the CC domain somehow stabilizes the helical content of the L2 region.

Further studies examining and assessing the L2 region α-helices in the context of a helical wheel diagram **(**Figure 4**)**, demonstrated that the N-terminal region displays a distinct amphipathic α-helix with a hydrophobic face[100]. Indeed, the N-terminal 32 amino acids of the L2 region comprise a primary sequence consistent with the existence of an amphipathic α-helix with a hydrophobic surface.

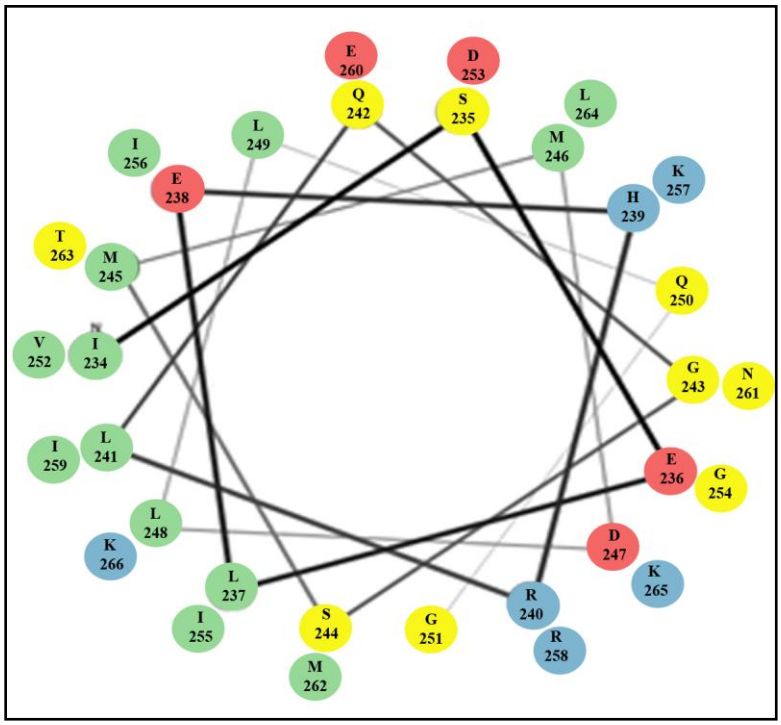

Figure 4: Helical wheel diagram of residues 263-285 of the N-terminal region of L2 on TRIM5α_{rh}. This depiction illustrates two interfaces in the L2 region. One interface principally comprises positively and negatively charged amino acids. The second interface consists of uncharged polar and non-polar amino acids. The N-terminal region displays a distinct amphipathic α-helix with a hydrophobic interface. Hydrophobic residues are shown in green, acidic residues are shown in red, basic residues are shown in blue, and polar residues are shown in yellow[100].

Proposed Models of TRIM5α Assembly

The Ganser-Pornillos Model (Figure 5)

Ganser-Pornillos et al. studied TRIM5 higher-order assembly using a TRIM5-21R chimeric protein where the RING domain of TRIM21 replaces the RING domain of TRIM5α_{rh} because it effectively restricts HIV-1 replication and is simpler to purify than wild-type TRIM5α[78]. This chimera spontaneously assembled into two-dimensional hexagonal arrays corresponding in symmetry and magnitudes to retroviral capsids, and this lattice formation does not require the SPRY domain[78]. However, TRIM5-21R assembly did require protein dimerization mediated by the CC domain as well as the surface exposed residue Arg121 in the B-box 2 domain[78]. Based on these results, the author's proposed a model for TRIM5α-mediated retroviral CA recognition that includes CA binding to the SPRY domain, TRIM5α dimerization, and assembly of a hexagonal lattice complementary to the CA lattice for avidity enhancement. Furthermore, this model proposes that the L2 regions of neighboring parallel dimers self-associate to organize TRIM5α assembly around the retroviral core.

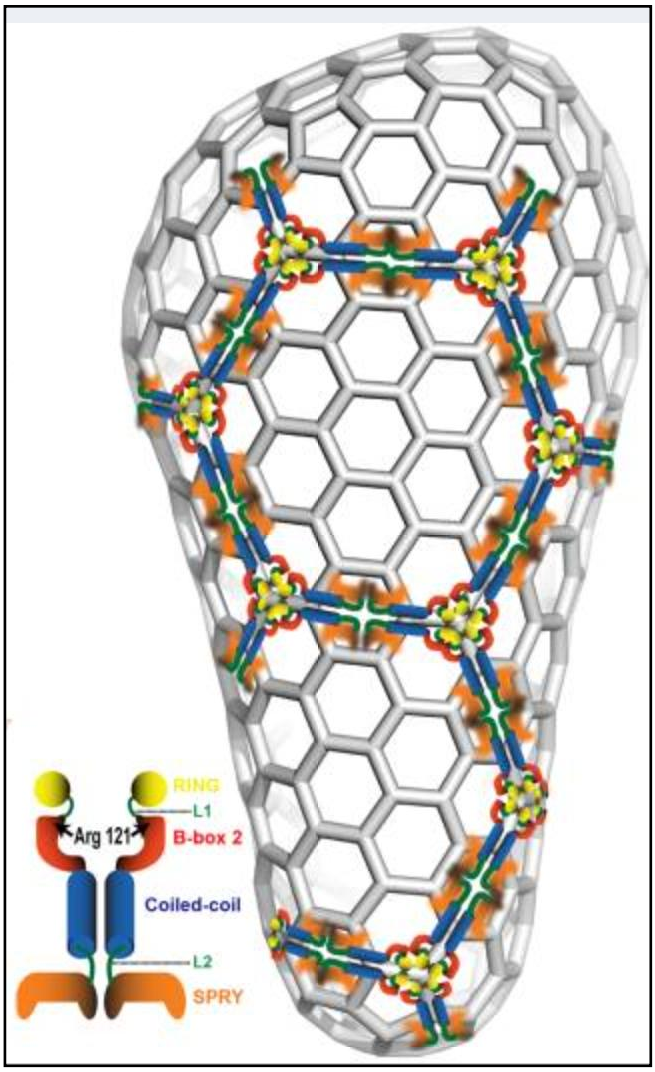

Figure 5: The Ganser-Pornillos model of TRIM5α assembly. Recombinant TRIM5-21R spontaneously assembles into two-dimensional paracrystalline hexagonal lattices. Binding to hexagonal arrays of the HIV-1 CA lattice triggers this assembly. TRIM5-21R assembly does not require the SPRY domain, however, it does require an Arg121 residue in the B-box 2 domain as well as protein dimerization. Additionally, the L2 regions of neighboring parallel dimers self-associate to facilitate assembly around the HIV-1 core. Reprinted with permission from[78].

The Sodroski Model (Figure 6)

Li et al. performed studies to further elucidate TRIM5α higher order self-association. Utilizing co-immunoprecipitation (CO-IP) assays, preformed TRIM5 dimers were able to CO-IP with homologous dimers forming higher order complexes, however this result diminished when the RING or RING-L1 domains were deleted, suggesting that the RING domain is required for higher order assembly but not dimerization[108]. In addition, TRIM5 dimers were able to CO-IP with heterologous dimers of closely related TRIM proteins (TRIM6 and TRIM34) although these interactions were weaker than their initial studies solely examining interactions of homologous dimers implying that higher order assembly of TRIM5 is governed by determinants in TRIM5 dimers[108]. Similar results were obtained when examining the role of the B-box 2 domain on higher order self-association. Disruption of the CC domain or elimination of the L2 region abolished TRIM5 higher order complex formation, which would support the idea that the formation of dimers must occur for further TRIM5 self-association[108]. Notably, Li et al. revealed that the SPRY domain of TRIM5α is not required for higher order complex formation as deletion of the SPRY domain had only very minimal effects on higher order assembly. In contrast, deletion or alteration of residues in the L2 region proximal to the CC domain elicited efficient dimerization but not higher order assembly of TRIM5α_{rh}[108]. The author's proposed a model suggesting that TRIM5 dimers, oriented in a parallel manner, form higher order complexes through RING and B-box 2 interactions at one end of the dimer and L2 regions at the other end of the dimer. The model suggests that TRIM5 forms a trimer of dimers that would allow for the formation of hexagonal arrays.

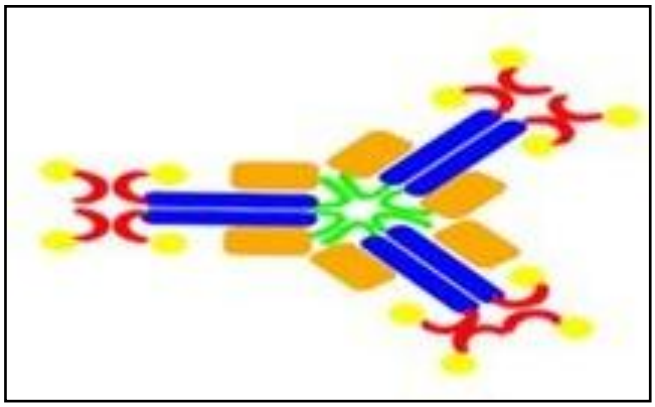

Figure 6: The Sodroski model of TRIM5α assembly. This model proposes that TRIM5α forms trimeric associations with parallel symmetry. Higher order self-association appears to be mediated by interactions between the RING (yellow) and B-box 2 (red) domains at one end of the dimer, and the L2 (green) region facilitates the formation of higher order complexes at the other end of the dimer. The SPRY (orange) domain appears dispensable for higher order self-association. The CC domain is shown in blue as a parallel dimer. Adapted from[100].

The Sanchez et al. Model (Figure 7)

Despite the findings mentioned above, the molecular details of TRIM oligomerization and high-order assembly are still poorly understood. A recent report by Sanchez et al. utilized biochemical and crystallographic analysis to determine that TRIM25 forms an elongated antiparallel dimer[109], in contrast to the model proposed by Ganser-pornillos et al. Human TRIM25 was used since it doesn't tend to form high-order assemblies, allowing for simpler use in biochemical assays. Crystallographic analysis of the TRIM25 CC domain and N-terminal half of the L2 region allowed visualization of a symmetrical dimer folding back into a hairpin configuration, in which the L2 region folds back and packs against alpha helix in the CC domain[109]. CC residues appeared to form a long arm of each subunit, indicated as helix H1, while the L2 residues appeared to form a short arm (containing helix H2 and H3) where H3 packs against an amphipathic platform formed by dimeric H1 interactions creating a 4-helix bundle[109].

Sanchez et al. also analyzed secondary structures across TRIM family members and determined that the presumed CC domains are fixed within an adjoining helix roughly 110 residues in length throughout the TRIM protein family, suggesting that the dimeric CC domain structure of other TRIM proteins (including TRIM5α) is conserved. Structural comparisons between TRIM5α and TRIM25 through disulfide crosslinking experiments determined that these two proteins have similar dimer constructions[109]. Through the experiments performed by Sanchez et al., it appears that each side of the TRIM5α hexagon is one CC dimer implying that the threefold symmetry of the hexagon

resembles the RING and B-box 2 domains, and the twofold symmetry of the hexagon corresponds to the SPRY domain[109]. These data suggest that the L2 region may stimulate the formation of cytoplasmic bodies and restriction by a previously unacknowledged mechanism.

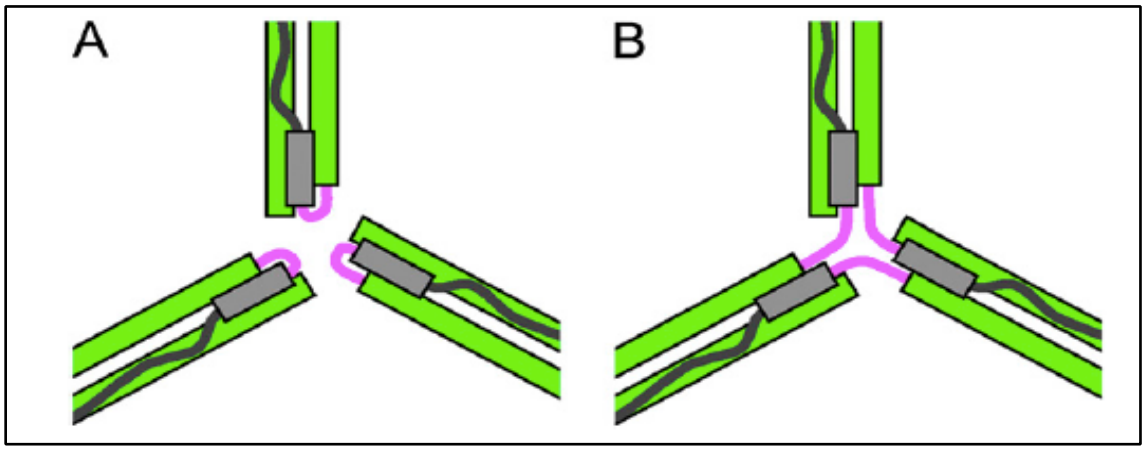

Figure 7: The Sanchez et al. model of TRIM5α assembly. Two potential arrangements of domain connectivity at the three-fold axes of the TRIM5α hexagonal lattice as observed by the TRIM25 crystal structure. (A) Three dimers with loops (magenta) connect the CC helices (green) and L2 (gray) by a fold-back mechanism. (B) Three dimers where the adjacent subunits have swapped their short arms. RING and B-box domains are not pictured. Reprinted with permission from[109].

Hypothesis

Proposed models of TRIM5α assembly, while speculative in nature, insinuate that the L2 region increases self-association and capsid binding. Our lab sought out conceivable mechanisms by which the L2 region might position the domains of TRIM5α_{rh}. We hypothesized that if the L2 region does not contribute to TRIM5α_{rh} self-association, then the Bbox2 domain must contribute all of the self-association activity of TRIM5α, and the only way in which a hexagonal assembly is intuitively possible in this case is in the setting of an antiparallel dimer[100]. We envisioned that the amphipathic helix in the N-terminal portion of the L2 region might fold back onto itself to form favorable interactions with other hydrophobic residues in the L2 region[100]. Biochemical cross-linking and fluorescence resonance energy transfer (FRET) analysis were utilized to distinguish between established models of TRIM5α assembly.

CHAPTER II

MATERIALS AND METHODS

Plasmids

The wild type TRIM5α_{rh} plasmid was a kind gift from Dr. Joseph Sodroski (Harvard school of Public Health). Polymerase chain reaction (PCR) utilizing primers specific for the CCL2 region, and the PCR product was digested with BamHI and XhoI to insert into pECFP-N1, pECFP-C1, pEYFP-N1, pEYFP-C1 (Clontech), which were also digested with BamHI and XhoI (Figure 8). The resulting constructs included: YFP-CCL2, CCL2-YFP, CFP-CCL2, and CCL2-CFP (Figure 13). A similar approach was taken in order to generate the CFP and YFP fused to the CC or L2 regions alone. All constructs were verified by sequencing and western blot to confirm expression of YFP and CFP.

Clone	Vector	Enzymes
YFP-CCL2	pEYFP-C1	BamHI/XhoI
CFP-CCL2	pECFP-C1	BamHI/XhoI
CCL2-YFP	pEYFP-N1	BamHI/XhoI
CCL2-CFP	pECFP-N1	BamHI/XhoI

Figure 8: Plasmid Cloning for FRET.

Western blotting

Cell lysates from transfected 293Ts were prepared by lysing cells in 1X NP-40 lysis buffer containing a protease inhibitor cocktail (PIC) on ice for 15 minutes. This was

followed by the addition of sodium dodecyl sulfate (SDS, final concentration of 1X SDS and boiling of samples at 100°C for 10 minutes to allow for protein denaturation. Equivalent amounts of protein were loaded onto a 10% polyacrylamide gel and subjected to SDS-polyacrylamide gel electrophoresis (SDS-PAGE) at 100V. Subsequently, proteins were transferred onto nitrocellulose membranes and probed with an anti-GFP primary antibody and an IgG horseradish peroxidase (HRP) secondary antibody. Western blots were identified using SuperSignal West Femto chemiluminescent substrate and a BioRad Chemidoc system[100].

Coomassie Staining

Purified protein samples were prepared by adding 2X SDS (for a final concentration of 1X SDS) and boiled at 100°C for 10 min. Equivalent amounts of protein were loaded onto a 10% polyacrylamide gel and subjected to SDS-PAGE at 100V. Afterwards, gels were fixed in a colloidal Coomassie fixative (45% methanol and 1% acetic acid in Milli Q water) for 1 hour and exposed to Coomassie stain (170 g ammonium sulfate, 1 g Coomassie G250, 0.5% acetic acid, and 34% methanol in Milli Q water) overnight. The following day, gels were washed with deionized water to remove excess stain and imaged with a BioRad Chemidoc system[100].

Glutaraldehyde Crosslinking

Cell lysates from transfected 293Ts were prepared by adding 100 µl of 1X lysis buffer + PIC to each sample and incubated on ice for 30 minutes. The samples were then spun down at 3,000 rpm for 1 minute to eliminate cellular debris and divided into 20 µl aliquots for cross-linking. Lysates were incubated with 0, 1, 2, and 4 mM glutaraldehyde

at room temperature for 5 minutes followed by saturation through the adding 2 µl of 1 M glycine to each sample (including samples that did not contain glutaraldehyde). Then, 20 µl of 2X-SDS was added to each sample and boiled at 100°C for 10 minutes. The cross-linked proteins were then loaded onto 4%-to-15% gradient Tris-HCl gels for SDS-PAGE and western blot analysis as described above. Purified proteins were treated in a similar manner but without 1X lysis buffer + PIC, and Coomassie staining was used instead of western blot analysis[100].

Fluorescence Resonance Energy Transfer (FRET)

Human embryonic kidney 293T cells were split into DeltaT dishes at 50% confluency and transfected, utilizing polyethylenimine (PEI), with 375ng total of YFP- or CFP-tagged CCL2 TRIM5α_{rh} in various combinations (discussed later). After 24 hours, FRET efficiency (E) was measured with a DeltaVision microscope equipped with a CoolSNAP HQ digital camera using a 60x objective lens. FRET efficiency was calculated by analyzing forty or more individual regions for each FRET pair using the following equation:

$$E = \frac{I_{DA} - a\,(I_{AA}) - d\,(I_{DD})}{I_{DA} - a\,(I_{AA}) + (G\text{-}d)(I_{DD})}$$

where I_{DD} is the intensity of fluorescence emission detected in the donor channel (470/30 nm) with 438/10 nm excitation; I_{AA} is the intensity of fluorescence emission detected in the acceptor channel with 559/27 nm emission and 513/12 nm excitation; I_{DA} is the

intensity of fluorescence emission detected in the "FRET" channel with 559/27 nm emission and 438/10 nm excitation. The "a" and "d" cross-talk coefficients were determined from acceptor-only or donor-only samples, respectively. The crosstalk coefficients were calculated utilizing the following equations:

$$a = \frac{I_{DA}}{I_{AA}}$$

$$d = \frac{I_{DA}}{I_{DD}}$$

We obtained a "d" value of 0.393 for CFP and an "a" value of 0.275 for YFP. G was calculated using a construct generously provided by Dr. Seth Robia, which contains 5 glycines flanked by CFP and YFP. YFP was progressively photo bleached while measuring the increase in CFP intensity. Once YFP was completely photo bleached, we measured the amount of donor recovery and determined G as the ratio of sensitized emission to the corresponding amount of donor recovery, which was 3.02[100].

CHAPTER III

RESULTS

Mutations in the L2 region that enhance the formation of cytoplasmic assemblies and HIV-1 restriction do not affect TRIM5α self-association

Previous data generated by Ganser-Pornillos et al. have revealed that TRIM5α assembles into 2-dimensional hexagonal arrays as described above[78]. However, the orientation of TRIM5α dimers in these hexagonal arrays remains poorly understood. Various models of TRIM5α assembly, illustrated in figure 9 (left and middle)**,** suggest that the dimers are oriented in a parallel fashion. These models further suggest that the L2 regions of TRIM5α dimers make contact with the L2 regions of opposing TRIM5α dimers in a manner that could enhance assembly by mediating the self-association of TRIM5α dimers. These findings along with our previous data, led us to hypothesize that mutations in the L2 region that enhance or reduce assembly would also affect the capability of TRIM5α_{rh} to self-associate. To test this hypothesis, we utilized biochemical cross-linking experiments to measure the self-association of TRIM5α_{rh} dimers and determine if the L2 region can mediate self-association *in vitro*. Both purified CCL2 peptide and CCL2 YFP or CFP fusion proteins were utilized in these experiments.

At low concentrations of glutaraldehyde (1 mM), a dimer was readily detectable with the CCL2 peptide (Figure 10). The dimer was also detected with TFH-AAA CCL2, RRV-AAA CCL2, and HKN-AAA CCL2 peptides and displayed striking similarities to

WT CCL2 peptide (Figure 10), suggesting that the ability of L2 to facilitate CC dimerization and the ability of L2 to affect TRIM5α_{rh} assembly are fundamentally independent of each other. As increasing concentrations of glutaraldehyde were used (2 and 4 mM), a laddering pattern emerged, consistent with nonspecific cross-linking of TRIM5α proteins. In all cases, and at all concentrations, we did not visualize any development of the tetrameric and hexameric species that would be suggestive of intrinsic self-association of CCL2 dimers[78, 108].

We also performed similar experiments with CCL2 fused to YFP, as described in the materials and methods. Here, we transfected 293T cells with the various constructs, collected the cell lysates, and subjected them to cross-linking experiments for western blot analysis. The CCL2 fusion proteins were cross-linked into a dimeric form in the presence of glutaraldehyde, similarly to recombinant CCL2 peptide experiments mentioned above (Figure 11).

Furthermore, we assessed the ability of L2 to facilitate self-association in the presence or absence of the CC domain. Again, this was done by cloning CC and L2 fragments alone into a YFP vector and subjected to glutaraldehyde cross-linking experiments. These experiments did not reveal any self-association activity of the L2 region alone, and no dimerization of the CC domain alone was visualized at any concentration of glutaraldehyde used (Figure 11). Therefore, it seems that the L2 region is not capable of intrinsic self-association, but it does seem to influence the ability of the CC region to dimerize. However, the ability of L2 to influence CC dimerization appears independent from its ability to affect assembly, since mutations previously described to affect

assembly of TRIM5α_{rh} formed dimers and higher-order multimers in cells. These data suggest that the L2 region is imperative for CC-mediated dimerization, which has also been demonstrated in previous studies[101].

In data generated previously in our lab, the RRV-AAA L2 mutant, which is unable to form cytoplasmic assemblies or restrict HIV-1, was shown to bind to *in vitro*-assembled HIV-1 capsids as efficiently as WT[100]. This proposes that the L2 region does not directly increase the self-association properties of TRIM5α_{rh} essential for capsid binding, implying that the L2 region does not directly contribute to the self-association of TRIM5α_{rh} dimers[100].

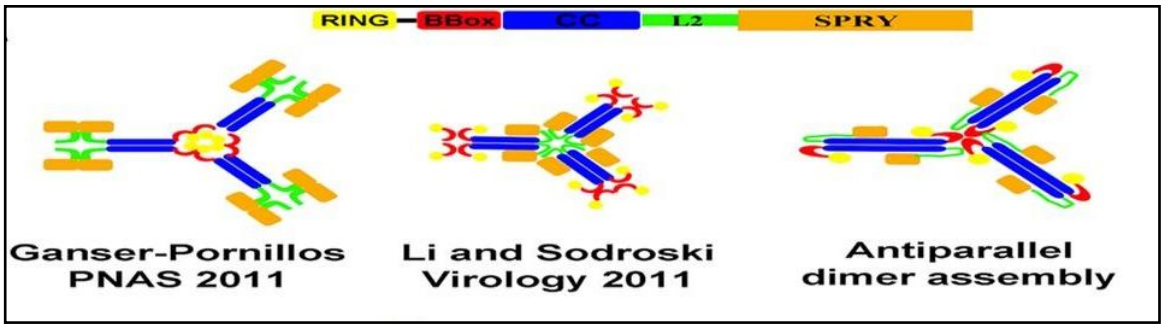

Figure 9: Published models of TRIM5 assembly. The various models of TRIM5α assembly are color-coordinated with the illustrated domain organization of TRIM5α. (Left) The Ganser-Pornillos model suggesting a parallel dimer assembly where the L2 regions of opposing dimers make direct contact. (Middle) The Li and Sodroski model also suggesting a parallel dimer assembly, however this model suggests the formation of a trimer of dimers. (Right) The Sanchez et al. model suggesting antiparallel dimer assembly where the L2 region folds back on itself to form favorable interactions between the amphipathic helix at the N-terminus of the L2 region and hydrophobic residues further downstream in the L2 region[100].

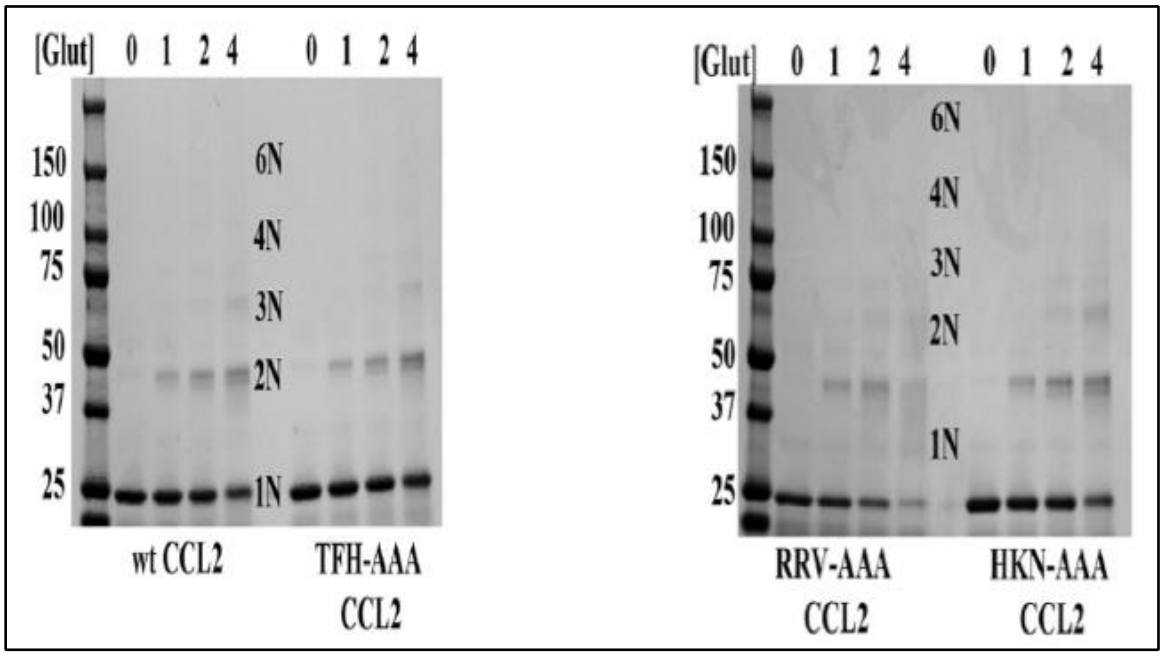

Figure 10: L2 mutations that enhance TRIM5α_{rh} assembly and HIV-1 restriction do not affect the ability of TRIM5α_{rh} to self-associate. The indicated CCL2 peptides were cross-linked at room temperature by using increasing amounts of glutaraldehyde for 5 min. The glutaraldehyde was saturated by the addition of 1 M glycine, and cross-linked peptides were visualized by SDS-PAGE and Coomassie staining[100].

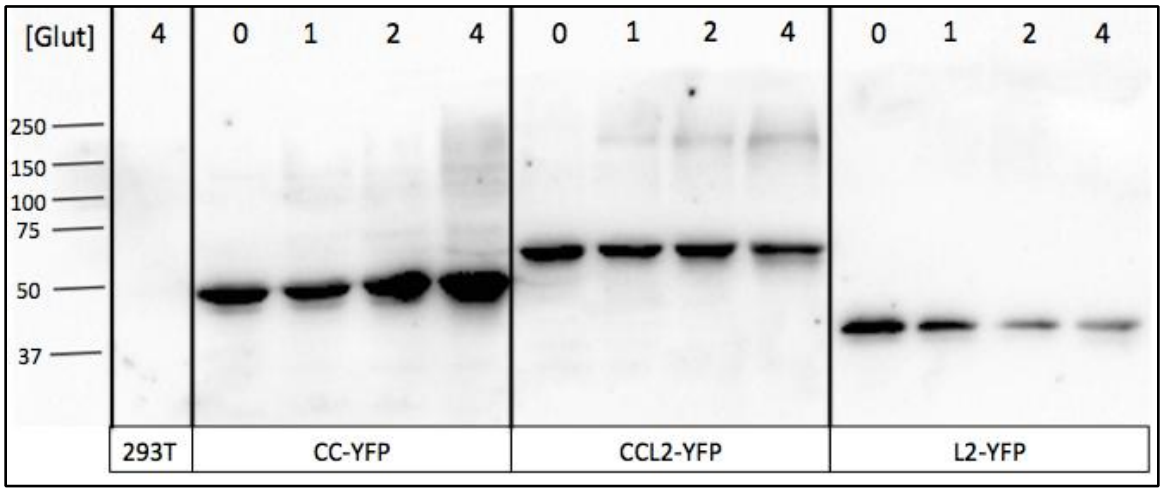

Figure 11: The L2 region influences the ability of the CC domain to dimerize. 293T cells were transfected with the indicated constructs and cell lysates were cross-linked in the presence of increasing concentrations of glutaraldehyde. The samples were then saturated with 1 M glycine and subjected to SDS-PAGE and western blot analysis using an anti-GFP primary antibody and IgG-HRP secondary antibody.

CHAPTER IV

RESULTS

FRET analysis reveals that TRIM5α forms antiparallel dimers

Consistent with our previous findings that demonstrate that the L2 region does not directly affect self-association of TRIM5α dimers, a recent study by Sanchez et al. reported the crystal structure of the TRIM25 CCL2 domain, which revealed that TRIM25 forms an elongated antiparallel dimer in which the L2 regions fold back along the helix of the CC dimer[109]. Additionally, structural and biochemical data have revealed that the CC domain and L2 region of both TRIM25 and TRIM5α form comparable structures[109]. We therefore tested the possibility that the CCL2 fragments of TRIM5α_{rh} similarly form antiparallel dimers (Figure 9, right) using FRET analysis.

FRET efficiency measurements are utilized to determine if two fluorophores are within a certain distance of each other. In order for these types of experiments to be valid, the distance between fluorophores must be smaller than 10 nm. A general depiction of how FRET operates is shown in figure 12[110]. The basic phenomenon of FRET is that a donor group is excited at a specific wavelength (unable to excite the acceptor) and absorbs the energy from this excitation. If the acceptor group is less than 10 nm away from the donor, then the energy from the donor will be transferred to the acceptor. This energy transfer leads to decreased donor fluorescence intensity and increased acceptor

emission fluorescence intensity. In order energy transfer to occur, the excitation wavelength spectrum of the acceptor group should overlap the emission wavelength spectrum of the acceptor group. The most commonly used fluorescent protein FRET pair is cyan fluorescent protein (CFP) and yellow fluorescent protein (YFP) since the CFP emission spectrum significantly overlaps the YFP excitation spectrum, supporting a strong FRET interaction.

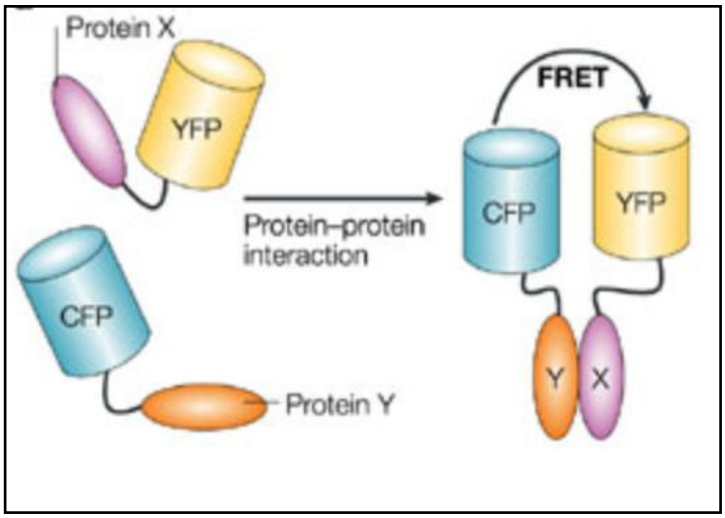

Figure 12: A general depiction of the molecular FRET mechanism. Two proteins (X and Y) are fused to YFP and CFP. The donor (CFP) is excited at the appropriate wavelength, and if the acceptor (YFP) is in close enough proximity, measurable energy will be transferred from donor to acceptor causing an increase in FRET efficiency. Reprinted with permission from[110].

To distinguish between the various models of TRIM5α assembly, we created CCL2 fusions to fluorescent YFP and CFP FRET pairs shown in figure 13. Both N- and C- terminal CFP and YFP fusions to CCL2 were generated since FRET efficiency displays a sixth-order dependence on the separation distance between fluorophores. By producing all four possible CCL2 fluorescent protein constructs (YFP-CCL2, CFP-CCL2, CCL2-YFP, and CCL2-CFP) we were able to investigate the relative orientation of fluorophores in CCL2 dimers using ensemble FRET measured in 293T cells transfected with various combinations of CCL2 CFP and YFP FRET pairs. The FRET efficiency was then calculated, as described in materials and methods, and compared amongst the various combinations of CCL2 YFP/CFP FRET pairs to differentiate between parallel and antiparallel dimer orientations of the CCL2 domain from TRIM5α_{rh}.

A schematic of the projected FRET efficiencies based on proposed models of TRIM5α dimerization is illustrated in figure 14. In the case of a CCL2 parallel dimer, the expected highest FRET efficiency would occur in the presence of CFP-CCL2 and YFP-CCL2, and the expected lowest FRET efficiency would occur in the presence of CCL2-CFP and YFP-CCL2. However, if CCL2 forms an antiparallel dimer, the highest FRET efficiency would occur in the presence of CCL2-CFP and CCL2-YFP, and the lowest FRET efficiency would occur in the presence of CFP-CCL2 and YFP-CCL2.

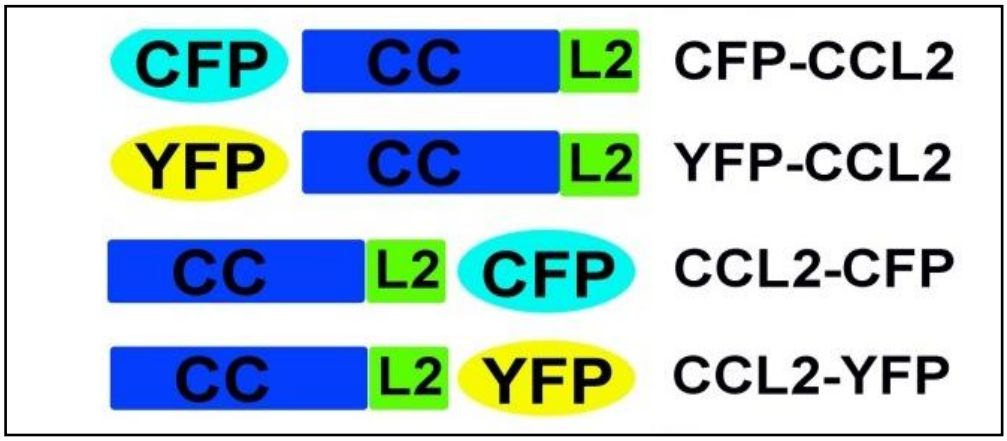

Figure 13: Schematic of constructs generated for FRET analysis. Constructs containing N-terminal and C-terminal YFP and CFP fused to CCL2 of TRIM5α_{rh} were created. The generation of all four conceivable constructs allowed us to differentiate between possible CCL2 domain orientations through analyses of all combinations of FRET pairs[100].

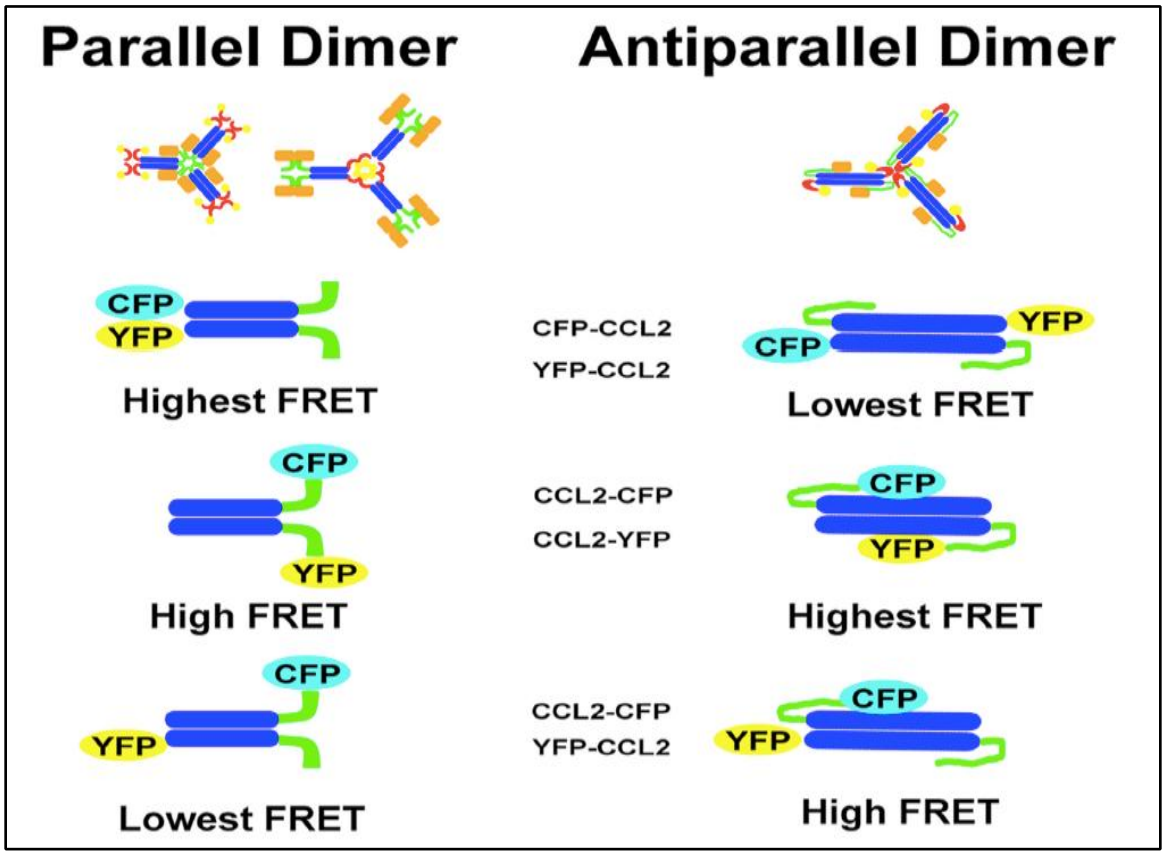

Figure 14: Expected FRET efficiencies based on the proposed models of TRIM5α. (Left) A parallel dimer orientation, as proposed in the Ganser-Pornillos and Sodroski model of TRIM5α, would be expected to give the highest FRET efficiency when CFP and YFP FRET pairs are on the N-terminus of the CCL2 domain and the lowest FRET efficiency when CFP and YFP are on the N- and C-terminus. (Right) An antiparallel dimer orientation, as proposed by Sanchez et al., would be expected to give the highest FRET efficiency when CFP and YFP FRET pairs are on the C-terminus of the CCL2 domain and the lowest FRET efficiency when CFP and YFP are on the N-terminus[100].

When the FRET efficiencies of all possible CCL2 CFP/YFP FRET pairs were compared, they suggested a pattern consistent with an antiparallel dimer that has been previously described for TRIM25[100, 109]. The calculated FRET efficiencies are shown in figure 16. At about 20%, the highest FRET efficiency corresponded to an orientation where both fluorophores were at the C-terminus of CCL2 (CCL2-CFP and CCL2-YFP)[100]. In contrast, the lowest FRET efficiency (at about 2%) was observed when both fluorophores were at the N-terminus of CCL2 (CFP-CCL2 and YFP-CCL2)[100]. An intermediate FRET efficiency (5-10%) was revealed when fluorophores were at opposite ends of CCL2 (CCL2-YFP/CFP-CCL2 or CCL2-CFP/YFP-CCL2)[100]. These data are consistent with the expected FRET efficiency pattern of an antiparallel dimer illustrated in figure 14. If a parallel dimer were predominant, then we would have expected to see the highest FRET efficiency in the presence of the N-terminal fusions to CFP and YFP. However, this was not observed suggesting that the CCL2 dimer has antiparallel symmetry allowing the L2 region to fold back down the CC helix giving the closest FRET pair configuration and, therefore, FRET efficiency[100].

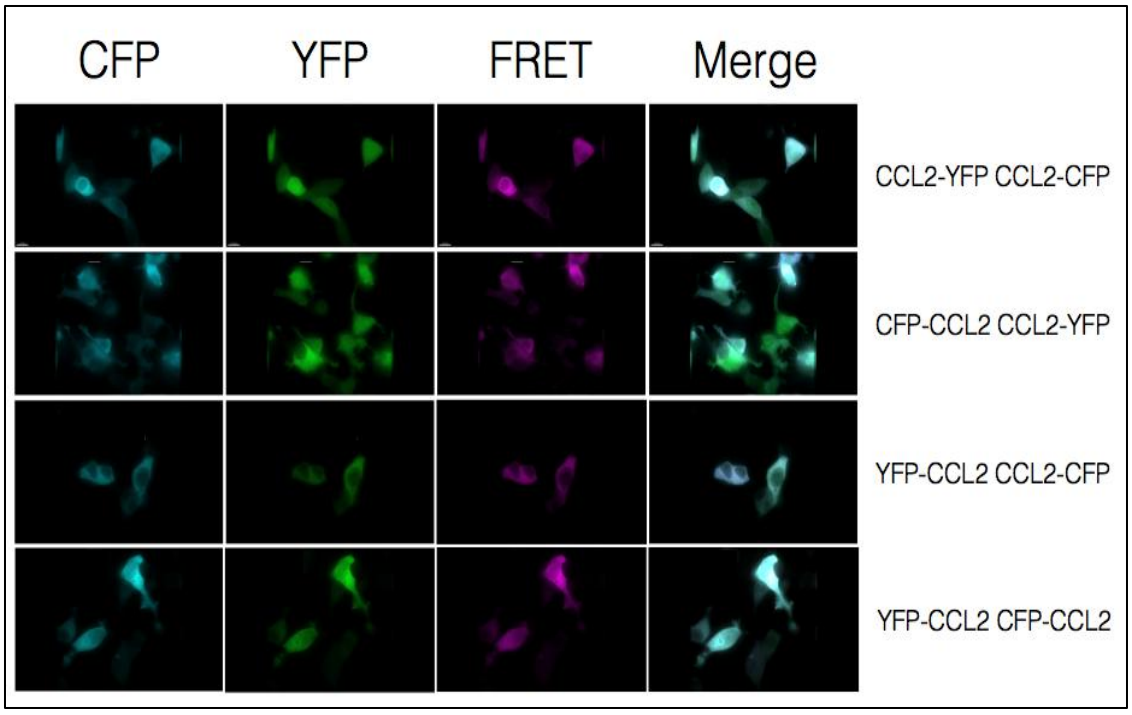

Figure 15: Representative Images from FRET Experiments. Human embryonic kidney 293T cells were split into DeltaT dishes at 50% confluency and transfected, utilizing polyethylenimine (PEI), with 375ng total of YFP- or CFP-tagged CCL2 TRIM5α_{rh} in various combinations. After 24 hours, FRET efficiency (E) was measured with a DeltaVision microscope equipped with a CoolSNAP HQ digital camera using a 60x objective lens. FRET efficiency was calculated by analyzing forty or more individual regions for each FRET pair. The scale bars are shown in the first row.

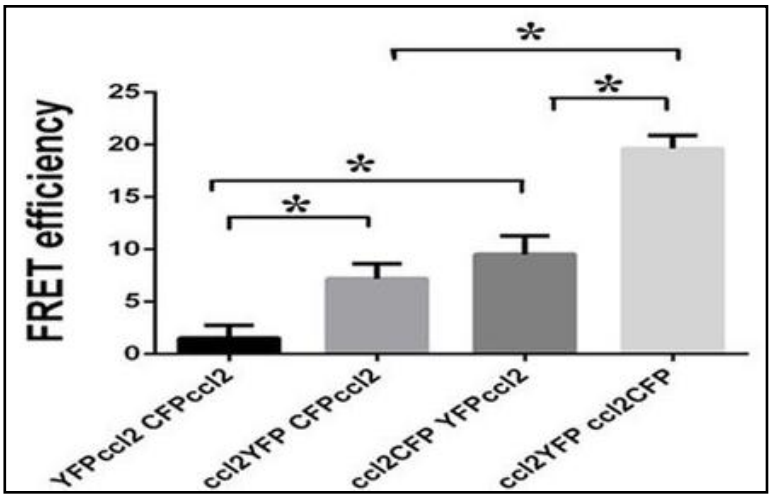

Figure 16: FRET analysis reveals that TRIM5α forms antiparallel dimers. The indicated combinations of CCL2 FRET pairs were transfected into 293T cells, and ensemble FRET efficiency was measured at 24 hours post-transfection. At least forty different regions were analyzed for each FRET pair to determine the fluorescence intensity of the donor, acceptor, and FRET channels. A *P* value of less than 0.001 was determined*. Results are representative of three independent experiments.[100].

CHAPTER V

DISCUSSION

The FRET experiments described above support the observation that TRIM proteins, specifically TRIM5α_{rh}, form antiparallel dimers. Based on our studies and the studies performed by Sanchez et al. we developed a homology model of the CCL2 fragment of TRIM5α_{rh} utilizing the recently reported structure of the TRIM25 CCL2 dimer. As illustrated in figure 17, our molecular modeling of the CCL2 region reveals intramolecular contacts critical for assembly and restriction[100]. Sanchez et al. described three helices (H1, H2, and H3) in the L2 region:

Helix 1: H1 covers the complete CC domain and a small portion of the L2 region. This appears to form the 'long arm' of each CCL2 subunit.

Helix 2: H2 interacts with H1 to create a hairpin or 'kink' in the L2 region that mediates the folding back of the L2 region onto the long arm of the CCL2 dimer.

Helix 3: H3 docks against H1 of the CC domain to form a 4-helix bundle. H2 and H3 appear to form the 'short arm' of each CCL2 subunit.

Similarly, our homology model indicates the presence of three α-helices in the L2 region of TRIM5α_{rh} that partake in important interactions in the antiparallel dimer (see figure 17). Mutations that abrogate assembly and restriction (KPK266-268AAA and RRV275-277AAA) are shown in figure 17 in red, while mutations that enhance assembly and

increase restriction (TFH269-271AAA and HKN271-273AAA) are depicted in green. Our biochemical cross-linking studies of purified recombinant WT CCL2 and the L2 variants showed no differences in dimerization, and none of the four peptides produced any species higher than a dimer (Figure 10). Additionally, cross-linking of just the L2 region or CC domain alone abolished dimerization (Figure 11). Interestingly, CD analysis of the L2 region alone, performed previously in our lab, revealed that the L2 region is disordered. Collectively, these data propose that the abilities of residues within the L2 region to facilitate CC domain dimerization and affect higher order self-association of TRIM5α_{rh} are fundamentally independent.

We believe that restriction and assembly mediated by TRIMα_{rh} essentially depends on H3 docking to H1 of the CC domain to form a 4-helix bundle. This is supported by previous studies in our lab that revealed that the TFH and HKN mutations display increased α-helical content in CCL2 dimers, while the RRV mutation had decreased α-helical content[100]. Our studies looking at the dynamics of the RRV mutant compared to the WT CCL2 dimer suggest that H3 is stabilized by interaction of the RRV motif with H1[100].

These data support our idea that there are three separate aspects of TRIM5α_{rh} self-association:

Dimerization: An antiparallel dimer is the basic unit of TRIM5α self-association. Formation is governed by interactions in the center of H1 of the CC domain (forming an amphipathic platform) and also by some elements of the L2 region.

This is supported by our inability to visualize dimeric species when just the CC domain or L2 region alone are cross-linked

Higher order self-association: This component of TRIM5α_{rh} self-association is facilitated by the B-box 2 domain. This is consistent with structural studies performed by Sanchez et al. along with our FRET analysis revealing that TRIM proteins form antiparallel dimers[100, 109] because, in the context of an antiparallel dimer, the only way to promote development of higher order complexes of TRIM5α_{rh} required for assembly of a hexameric lattice is if the B-box 2 domain is situated at either end of the antiparallel dimer. Our observation that L2 mutations do not alter higher order self-association in cross-linking experiments further support this notion[100].

Assembly: Assembly is mediated by C-terminal elements in the L2 region, which could have an influence on proper spacing of SPRY domains to recognize the HIV-1 core. Indeed, Ganser-Pornillos et al. and Sanchez et al. have previously suggested this idea. Previous data published from our lab further supports this by showing that alterations of the L2 region affected assembly without affecting capsid binding[99, 100]. These data suggest that the L2 region has a previously unappreciated step in assembly of TRIM5α_{rh} prior to binding the HIV-1 capsid[100].

Shortly after we published our findings that the L2 region contains determinants important for antiparallel dimer formation and assembly, a study by Goldstone et al. was published showing that TRIM5α forms an antiparallel dimer that permits binding to the

HIV-1 capsid lattice[111]. Their group determined the crystal structure of the B-box2 and CC domain displaying the elongated antiparallel dimers of CC domains. As previously hypothesized, the crystal structure reveals that the B-box2 domains can be positioned at either end of the CC domain through interactions with a helix in the L2 region of the opposing monomer[111]. From these structural studies, Goldstone et al. concluded that the antiparallel symmetry of TRIM5α facilitate the proper positioning of N- and C-terminal domains, which promotes stable binding to the hexameric lattice of the HIV-1 viral core.

Based on the studies performed by our lab, Sanchez et al. and Goldstone et al., it appears that the new 'dogma' of TRIM5α self-association is in the context of an antiparallel dimer. This would argue against the models proposed by Ganser-Pornillos et al. and Li et al. described earlier. Continued studies are important in order to understand the molecular mechanism of L2-mediated self-association events, which may provide insight into the precise mechanism of TRIM5α_{rh}-mediated HIV-1 capsid disassembly to allow for restriction process.

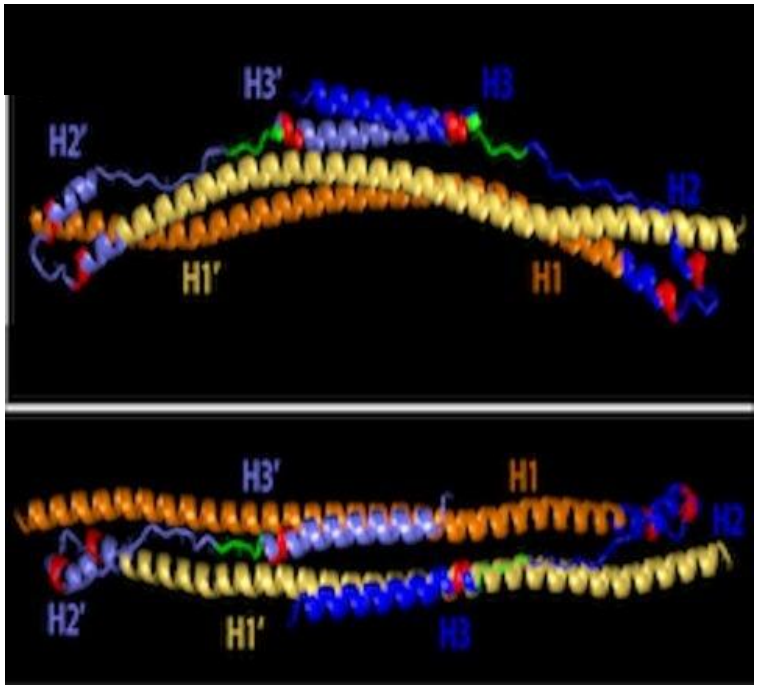

Figure 17: Model of the TRIM5α_{rh} CCL2 dimer. The CC domains are colored orange. The L2 regions are depicted in blue. Assembly- and HIV-1 restriction-disrupting mutations (as previously described) are shown in red. Assembly- and restriction-enhancing mutations are illustrated in green. The three proposed helices, based off of studies performed by Sanchez et al., are also indicated. The opposing monomer is a lighter shade for simplicity[100].

REFERENCE LIST

1. Ganser, B.K., et al., *Assembly and analysis of conical models for the HIV-1 core.* Science, 1999. **283**(5398): p. 80-3.

2. Ganser-Pornillos, B.K., M. Yeager, and W.I. Sundquist, *The structural biology of HIV assembly.* Curr Opin Struct Biol, 2008. **18**(2): p. 203-17.

3. Robinson, H.L., *New hope for an AIDS vaccine.* Nat Rev Immunol, 2002. **2**(4): p. 239-50.

4. Engelman, A. and P. Cherepanov, *The structural biology of HIV-1: mechanistic and therapeutic insights.* Nat Rev Microbiol, 2012. **10**(4): p. 279-90.

5. Bukrinsky, M.I., et al., *Association of integrase, matrix, and reverse transcriptase antigens of human immunodeficiency virus type 1 with viral nucleic acids following acute infection.* Proc Natl Acad Sci U S A, 1993. **90**(13): p. 6125-9.

6. Farnet, C.M. and W.A. Haseltine, *Determination of viral proteins present in the human immunodeficiency virus type 1 preintegration complex.* J Virol, 1991. **65**(4): p. 1910-5.

7. Miller, M.D., C.M. Farnet, and F.D. Bushman, *Human immunodeficiency virus type 1 preintegration complexes: studies of organization and composition.* J Virol, 1997. **71**(7): p. 5382-90.

8. Yamashita, M. and M. Emerman, *Capsid is a dominant determinant of retrovirus infectivity in nondividing cells.* J Virol, 2004. **78**(11): p. 5670-8.

9. De Iaco, A., et al., *TNPO3 protects HIV-1 replication from CPSF6-mediated capsid stabilization in the host cell cytoplasm.* Retrovirology, 2013. **10**: p. 20.

10. Di Nunzio, F., et al., *Human nucleoporins promote HIV-1 docking at the nuclear pore, nuclear import and integration.* PLoS One, 2012. **7**(9): p. e46037.

11. Di Nunzio, F., et al., *Nup153 and Nup98 bind the HIV-1 core and contribute to the early steps of HIV-1 replication.* Virology, 2013. **440**(1): p. 8-18.

12. Krishnan, L., et al., *The requirement for cellular transportin 3 (TNPO3 or TRN-SR2) during infection maps to human immunodeficiency virus type 1 capsid and not integrase.* J Virol, 2010. **84**(1): p. 397-406.

13. Collier, A.C., et al., *Treatment of human immunodeficiency virus infection with saquinavir, zidovudine, and zalcitabine. AIDS Clinical Trials Group.* N Engl J Med, 1996. **334**(16): p. 1011-7.

14. Autran, B., et al., *Positive effects of combined antiretroviral therapy on CD4+ T cell homeostasis and function in advanced HIV disease.* Science, 1997. **277**(5322): p. 112-6.

15. Komanduri, K.V., et al., *Restoration of cytomegalovirus-specific CD4+ T-lymphocyte responses after ganciclovir and highly active antiretroviral therapy in individuals infected with HIV-1.* Nat Med, 1998. **4**(8): p. 953-6.

16. Lederman, M.M., et al., *Immunologic responses associated with 12 weeks of combination antiretroviral therapy consisting of zidovudine, lamivudine, and ritonavir: results of AIDS Clinical Trials Group Protocol 315.* J Infect Dis, 1998. **178**(1): p. 70-9.

17. Arts, E.J. and D.J. Hazuda, *HIV-1 antiretroviral drug therapy.* Cold Spring Harb Perspect Med, 2012. **2**(4): p. a007161.

18. Kwong, P.D., et al., *Structure of an HIV gp120 envelope glycoprotein in complex with the CD4 receptor and a neutralizing human antibody.* Nature, 1998. **393**(6686): p. 648-59.

19. Madani, N., et al., *Small-molecule CD4 mimics interact with a highly conserved pocket on HIV-1 gp120.* Structure, 2008. **16**(11): p. 1689-701.

20. Wu, X., et al., *Rational design of envelope identifies broadly neutralizing human monoclonal antibodies to HIV-1.* Science, 2010. **329**(5993): p. 856-61.

21. Wu, X., et al., *Focused evolution of HIV-1 neutralizing antibodies revealed by structures and deep sequencing.* Science, 2011. **333**(6049): p. 1593-602.

22. Eckert, D.M. and P.S. Kim, *Design of potent inhibitors of HIV-1 entry from the gp41 N-peptide region.* Proc Natl Acad Sci U S A, 2001. **98**(20): p. 11187-92.

23. Wild, C.T., et al., *Peptides corresponding to a predictive alpha-helical domain of human immunodeficiency virus type 1 gp41 are potent inhibitors of virus infection.* Proc Natl Acad Sci U S A, 1994. **91**(21): p. 9770-4.

24. Arion, D., et al., *Phenotypic mechanism of HIV-1 resistance to 3'-azido-3'-deoxythymidine (AZT): increased polymerization processivity and enhanced sensitivity to pyrophosphate of the mutant viral reverse transcriptase.* Biochemistry, 1998. **37**(45): p. 15908-17.

25. Meyer, P.R., et al., *A mechanism of AZT resistance: an increase in nucleotide-dependent primer unblocking by mutant HIV-1 reverse transcriptase.* Mol Cell, 1999. **4**(1): p. 35-43.

26. Kohlstaedt, L.A., et al., *Crystal structure at 3.5 A resolution of HIV-1 reverse transcriptase complexed with an inhibitor.* Science, 1992. **256**(5065): p. 1783-90.

27. Ren, J., et al., *High resolution structures of HIV-1 RT from four RT-inhibitor complexes.* Nat Struct Biol, 1995. **2**(4): p. 293-302. 28. Das, K., et al., *High-resolution structures of HIV-1 reverse transcriptase/TMC278 complexes: strategic flexibility explains potency against resistance mutations.* Proc Natl Acad Sci U S A, 2008. **105**(5): p. 1466-71.

28. Das, K., et al., *High-resolution structures of HIV-1 reverse transcriptase/TMC278 complexes: strategic flexibility explains potency against resistance mutations.* Proc Natl Acad Sci U S A, 2008. **105**(5): p. 1466-71.

29. Hare, S., et al., *Molecular mechanisms of retroviral integrase inhibition and the evolution of viral resistance.* Proc Natl Acad Sci U S A, 2010. **107**(46): p. 20057-62.

30. Hare, S., et al., *Retroviral intasome assembly and inhibition of DNA strand transfer.* Nature, 2010. **464**(7286): p. 232-6.

31. Espeseth, A.S., et al., *HIV-1 integrase inhibitors that compete with the target DNA substrate define a unique strand transfer conformation for integrase.* Proc Natl Acad Sci U S A, 2000. **97**(21): p. 11244-9.

32. Maertens, G.N., S. Hare, and P. Cherepanov, *The mechanism of retroviral integration from X-ray structures of its key intermediates.* Nature, 2010. **468**(7321): p. 326-9.

33. Christ, F., et al., *Rational design of small-molecule inhibitors of the LEDGF/p75-integrase interaction and HIV replication.* Nat Chem Biol, 2010. **6**(6): p. 442-8.

34. Bieniasz, P.D., *Intrinsic immunity: a front-line defense against viral attack.* Nat Immunol, 2004. **5**(11): p. 1109-15.

35. Lilly, F., *Susceptibility to two strains of Friend leukemia virus in mice.* Science, 1967. **155**(3761): p. 461-2.

36. Towers, G., et al., *A conserved mechanism of retrovirus restriction in mammals.* Proc Natl Acad Sci U S A, 2000. **97**(22): p. 12295-9.

37. Malim, M.H. and P.D. Bieniasz, *HIV Restriction Factors and Mechanisms of Evasion.* Cold Spring Harb Perspect Med, 2012. **2**(5): p. a00694.

38. Sheehy, A.M., et al., *Isolation of a human gene that inhibits HIV-1 infection and is suppressed by the viral Vif protein.* Nature, 2002. **418**(6898): p. 646-50.

39. Harris, R.S., et al., *DNA deamination mediates innate immunity to retroviral infection.* Cell, 2003. **113**(6): p. 803-9.

40. Albin, J.S. and R.S. Harris, *Interactions of host APOBEC3 restriction factors with HIV-1 in vivo: implications for therapeutics.* Expert Rev Mol Med, 2010. **12**: p. e4.

41. Malim, M.H., *APOBEC proteins and intrinsic resistance to HIV-1 infection.* Philos Trans R Soc Lond B Biol Sci, 2009. **364**(1517): p. 675-87.

42. Hrecka, K., et al., *Vpx relieves inhibition of HIV-1 infection of macrophages mediated by the SAMHD1 protein.* Nature, 2011. **474**(7353): p. 658-61.

43. Laguette, N., et al., *SAMHD1 is the dendritic- and myeloid-cell-specific HIV-1 restriction factor counteracted by Vpx.* Nature, 2011. **474**(7353): p. 654-7.

44. Ayinde, D., N. Casartelli, and O. Schwartz, *Restricting HIV the SAMHD1 way: through nucleotide starvation.* Nat Rev Microbiol, 2012. **10**(10): p. 675-80.

45. Laguette, N. and M. Benkirane, *How SAMHD1 changes our view of viral restriction.* Trends Immunol, 2012. **33**(1): p. 26-33.

46. Laguette, N., et al., *Evolutionary and functional analyses of the interaction between the myeloid restriction factor SAMHD1 and the lentiviral Vpx protein.* Cell Host Microbe, 2012. **11**(2): p. 205-17.

47. Lim, E.S., et al., *The ability of primate lentiviruses to degrade the monocyte restriction factor SAMHD1 preceded the birth of the viral accessory protein Vpx.* Cell Host Microbe, 2012. **11**(2): p. 194-204.

48. Nobile, C., et al., *Covert human immunodeficiency virus replication in dendritic cells and in DC-SIGN-expressing cells promotes long-term transmission to lymphocytes.* J Virol, 2005. **79**(9): p. 5386-99.

49. Neil, S.J., et al., *HIV-1 Vpu promotes release and prevents endocytosis of nascent retrovirus particles from the plasma membrane.* PLoS Pathog, 2006. **2**(5): p. e39.

50. Neil, S.J., et al., *An interferon-alpha-induced tethering mechanism inhibits HIV-1 and Ebola virus particle release but is counteracted by the HIV-1 Vpu protein.* Cell Host Microbe, 2007. **2**(3): p. 193-203.

51. Van Damme, N., et al., *The interferon-induced protein BST-2 restricts HIV-1 release and is downregulated from the cell surface by the viral Vpu protein.* Cell Host Microbe, 2008. **3**(4): p. 245-52.

52. Perez-Caballero, D., et al., *Tetherin inhibits HIV-1 release by directly tethering virions to cells.* Cell, 2009. **139**(3): p. 499-511.

53. Neil, S.J., T. Zang, and P.D. Bieniasz, *Tetherin inhibits retrovirus release and is antagonized by HIV-1 Vpu.* Nature, 2008. **451**(7177): p. 425-30.

54. Jouvenet, N., et al., *Broad-spectrum inhibition of retroviral and filoviral particle release by tetherin.* J Virol, 2009. **83**(4): p. 1837-44.

55. Fitzpatrick, K., et al., *Direct restriction of virus release and incorporation of the interferon-induced protein BST-2 into HIV-1 particles.* PLoS Pathog, 2010. **6**(3): p. e1000701.

56. Hammonds, J., et al., *Immunoelectron microscopic evidence for Tetherin/BST2 as the physical bridge between HIV-1 virions and the plasma membrane.* PLoS Pathog, 2010. **6**(2): p. e1000749.

57. Dube, M., et al., *Antagonism of tetherin restriction of HIV-1 release by Vpu involves binding and sequestration of the restriction factor in a perinuclear compartment.* PLoS Pathog, 2010. **6**(4): p. e1000856.

58. Mitchell, R.S., et al., *Vpu antagonizes BST-2-mediated restriction of HIV-1 release via beta-TrCP and endo-lysosomal trafficking.* PLoS Pathog, 2009. **5**(5): p. e1000450.

59. Bartee, E., A. McCormack, and K. Fruh, *Quantitative membrane proteomics reveals new cellular targets of viral immune modulators.* PLoS Pathog, 2006. **2**(10): p. e107.

60. Gupta, R.K., et al., *Mutation of a single residue renders human tetherin resistant to HIV-1 Vpu-mediated depletion.* PLoS Pathog, 2009. **5**(5): p. e1000443.

61. McNatt, M.W., et al., *Species-specific activity of HIV-1 Vpu and positive selection of tetherin transmembrane domain variants.* PLoS Pathog, 2009. **5**(2): p. e1000300.

62. Hatziioannou, T., et al., *Retrovirus resistance factors Ref1 and Lv1 are species-specific variants of TRIM5alpha.* Proc Natl Acad Sci U S A, 2004. **101**(29): p. 10774-9.

63. Keckesova, Z., L.M. Ylinen, and G.J. Towers, *The human and African green monkey TRIM5alpha genes encode Ref1 and Lv1 retroviral restriction factor activities.* Proc Natl Acad Sci U S A, 2004. **101**(29): p. 10780-5.

64. Perron, M.J., et al., *TRIM5alpha mediates the postentry block to N-tropic murine leukemia viruses in human cells.* Proc Natl Acad Sci U S A, 2004. **101**(32): p. 11827-32.

65. Stremlau, M., et al., *The cytoplasmic body component TRIM5alpha restricts HIV-1 infection in Old World monkeys.* Nature, 2004. **427**(6977): p. 848-53.

66. Perez-Caballero, D., et al., *Human tripartite motif 5alpha domains responsible for retrovirus restriction activity and specificity.* J Virol, 2005. **79**(14): p. 8969-78.

67. Sawyer, S.L., et al., *Positive selection of primate TRIM5alpha identifies a critical species-specific retroviral restriction domain.* Proc Natl Acad Sci U S A, 2005. **102**(8): p. 2832-7.

68. Stremlau, M., et al., *Species-specific variation in the B30.2(SPRY) domain of TRIM5alpha determines the potency of human immunodeficiency virus restriction.* J Virol, 2005. **79**(5): p. 3139-45.

69. Yap, M.W., S. Nisole, and J.P. Stoye, *A single amino acid change in the SPRY domain of human Trim5alpha leads to HIV-1 restriction.* Curr Biol, 2005. **15**(1): p. 73-8.

70. Sayah, D.M., et al., *Cyclophilin A retrotransposition into TRIM5 explains owl monkey resistance to HIV-1.* Nature, 2004. **430**(6999): p. 569-73.

71. Nisole, S., et al., *A Trim5-cyclophilin A fusion protein found in owl monkey kidney cells can restrict HIV-1.* Proc Natl Acad Sci U S A, 2004. **101**(36): p. 13324-8.

72. Stoye, J.P. and M.W. Yap, *Chance favors a prepared genome.* Proc Natl Acad Sci U S A, 2008. **105**(9): p. 3177-8.

73. Diaz-Griffero, F., et al., *Requirements for capsid-binding and an effector function in TRIMCyp-mediated restriction of HIV-1.* Virology, 2006. **351**(2): p. 404-19.

74. Kutluay, S.B., D. Perez-Caballero, and P.D. Bieniasz, *Fates of retroviral core components during unrestricted and TRIM5-restricted infection.* PLoS Pathog, 2013. **9**(3): p. e1003214.

75. Carthagena, L., et al., *Implication of TRIM alpha and TRIMCyp in interferon-induced anti-retroviral restriction activities.* Retrovirology, 2008. **5**: p. 59.

76. Javanbakht, H., et al., *The ability of multimerized cyclophilin A to restrict retrovirus infection.* Virology, 2007. **367**(1): p. 19-29.

77. Stremlau, M., et al., *Specific recognition and accelerated uncoating of retroviral capsids by the TRIM5alpha restriction factor.* Proc Natl Acad Sci U S A, 2006. **103**(14): p. 5514-9.

78. Ganser-Pornillos, B.K., et al., *Hexagonal assembly of a restricting TRIM5alpha protein.* Proc Natl Acad Sci U S A, 2011. **108**(2): p. 534-9.

79. Pertel, T., et al., *TRIM5 is an innate immune sensor for the retrovirus capsid lattice.* Nature, 2011. **472**(7343): p. 361-5.

80. Nisole, S., J.P. Stoye, and A. Saib, *TRIM family proteins: retroviral restriction and antiviral defence.* Nat Rev Microbiol, 2005. **3**(10): p. 799-808.

81. Reymond, A., et al., *The tripartite motif family identifies cell compartments.* EMBO J, 2001. **20**(9): p. 2140-51.

82. Meroni, G. and G. Diez-Roux, *TRIM/RBCC, a novel class of 'single protein RING finger' E3 ubiquitin ligases.* Bioessays, 2005. **27**(11): p. 1147-57.

83. James, L.C., et al., *Structural basis for PRYSPRY-mediated tripartite motif (TRIM) protein function.* Proc Natl Acad Sci U S A, 2007. **104**(15): p. 6200-5.

84. Yamauchi, K., et al., *Ubiquitination of E3 ubiquitin ligase TRIM5 alpha and its potential role.* FEBS J, 2008. **275**(7): p. 1540-55.

85. Ikeda, K. and S. Inoue, *TRIM proteins as RING finger E3 ubiquitin ligases.* Adv Exp Med Biol, 2012. **770**: p. 27-3

86. Gack, M.U., et al., *TRIM25 RING-finger E3 ubiquitin ligase is essential for RIG-I-mediated antiviral activity.* Nature, 2007. **446**(7138): p. 916-920.

87. Li, X., et al., *Functional replacement of the RING, B-box 2, and coiled-coil domains of tripartite motif 5alpha (TRIM5alpha) by heterologous TRIM domains.* J Virol, 2006. **80**(13): p. 6198-206.

88. Li, X., et al., *Virus-specific effects of TRIM5alpha(rh) RING domain functions on restriction of retroviruses.* J Virol, 2013. **87**(13): p. 7234-45.

89. Li, X. and J. Sodroski, *The TRIM5alpha B-box 2 domain promotes cooperative binding to the retroviral capsid by mediating higher-order self-association.* J Virol, 2008. **82**(23): p. 11495-502.

90. Javanbakht, H., et al., *The contribution of RING and B-box 2 domains to retroviral restriction mediated by monkey TRIM5alpha.* J Biol Chem, 2005. **280**(29): p. 26933-40.

91. Perron, M.J., et al., *The human TRIM5alpha restriction factor mediates accelerated uncoating of the N-tropic murine leukemia virus capsid.* J Virol, 2007. **81**(5): p. 2138-48.

92. Javanbakht, H., et al., *Characterization of TRIM5alpha trimerization and its contribution to human immunodeficiency virus capsid binding.* Virology, 2006. **353**(1): p. 234-46.

93. Maegawa, H., et al., *Contribution of RING domain to retrovirus restriction by TRIM5alpha depends on combination of host and virus.* Virology, 2010. **399**(2): p. 212-20.

94. Ohkura, S., et al., *All three variable regions of the TRIM5alpha B30.2 domain can contribute to the specificity of retrovirus restriction.* J Virol, 2006. **80**(17): p. 8554-65.

95. Song, B., et al., *The B30.2(SPRY) domain of the retroviral restriction factor TRIM5alpha exhibits lineage-specific length and sequence variation in primates.* J Virol, 2005. **79**(10): p. 6111-21.

96. Campbell, E.M., et al., *TRIM5 alpha cytoplasmic bodies are highly dynamic structures.* Mol Biol Cell, 2007. **18**(6): p. 2102-11.

97. Song, B., et al., *TRIM5alpha association with cytoplasmic bodies is not required for antiretroviral activity.* Virology, 2005. **343**(2): p. 201-11.

98. Campbell, E.M., et al., *Visualization of a proteasome-independent intermediate during restriction of HIV-1 by rhesus TRIM5alpha.* J Cell Biol, 2008. **180**(3): p. 549-61.

99. Sastri, J., et al., *Identification of residues within the L2 region of rhesus TRIM5alpha that are required for retroviral restriction and cytoplasmic body localization.* Virology, 2010. **405**(1): p. 259-66.

100. Sastri, J., et al., *Restriction of HIV-1 by Rhesus TRIM5alpha Is Governed by Alpha Helices in the Linker2 Region.* J Virol, 2014. **88**(16): p. 8911-23.

101. Mische, C.C., et al., *Retroviral restriction factor TRIM5alpha is a trimer.* J Virol, 2005. **79**(22): p. 14446-50.

102. Langelier, C.R., et al., *Biochemical characterization of a recombinant TRIM5alpha protein that restricts human immunodeficiency virus type 1 replication.* J Virol, 2008. **82**(23): p. 11682-94.

103. Kar, A.K., et al., *Biochemical and biophysical characterization of a chimeric TRIM21-TRIM5alpha protein.* J Virol, 2008. **82**(23): p. 11669-81.

104. Yap, M.W., et al., *Trim5alpha protein restricts both HIV-1 and murine leukemia virus.* Proc Natl Acad Sci U S A, 2004. **101**(29): p. 10786-91.

105. Diaz-Griffero, F., et al., *A B-box 2 surface patch important for TRIM5alpha self-association, capsid binding avidity, and retrovirus restriction.* J Virol, 2009. **83**(20): p. 10737-51.

106. Li, X., et al., *Functional interplay between the B-box 2 and the B30.2(SPRY) domains of TRIM5alpha.* Virology, 2007. **366**(2): p. 234-44.

107. Yap, M.W., et al., *The design of artificial retroviral restriction factors.* Virology, 2007. **365**(2): p. 302-14.

108. Li, X., et al., *Determinants of the higher order association of the restriction factor TRIM5alpha and other tripartite motif (TRIM) proteins.* J Biol Chem, 2011. **286**(32): p. 27959-70.

109. Sanchez, J.G., et al., *The tripartite motif coiled-coil is an elongated antiparallel hairpin dimer.* Proc Natl Acad Sci U S A, 2014. **111**(7): p. 2494-9.

110. Zhang, J., et al., *Creating new fluorescent probes for cell biology.* Nat Rev Mol Cell Biol, 2002. **3**(12): p. 906-18.

111. Goldstone, D.C., et al., *Structural studies of postentry restriction factors reveal antiparallel dimers that enable avid binding to the HIV-1 capsid lattice.* Proc Natl Acad Sci U S A, 2014. **111**(26): p. 9609-14.

VITA

The author, Laura Johnsen was born in Chicago, Illinois on November 10, 1989 to Dana Johnsen and Elizabeth Schultz. She received a Bachelor of Science from the University of Arizona (Tucson, Arizona) in May of 2012.

During her undergraduate college career, Laura became interested in studying microbiology and decided to continue her education in that field. In August of 2012, Laura joined the Department of Microbiology and Immunology at Loyola University Medical Center (Maywood, IL). Within the first couple of months, she joined the laboratory of Dr. Edward Campbell, where she studied a protein called Rhesus TRIM5alpha, which can restrict HIV-1 in Old World Monkeys but not humans.

After completing her Master of Science, Laura will continue on to pursue a Ph.D in a field related to environmental science.